Sound propagation in disordered media

sound as a probe: material acoustic characterization

Nicolás Mujica
Departamento de Física (DFI)
Facultad de Ciencias Físicas y Matemáticas (FCFM)
Universidad de Chile

Introduction: wave propagation in disordered media

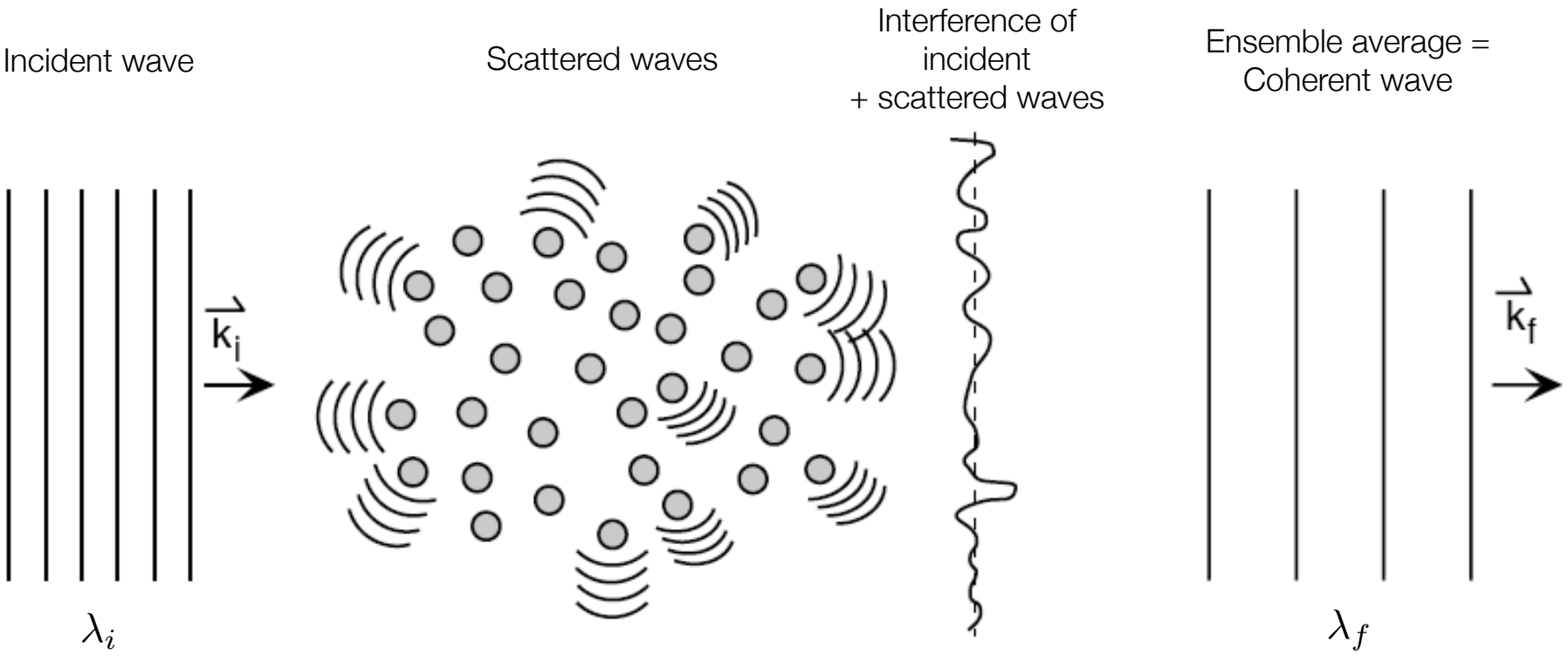

Introduction: wave propagation in disordered media

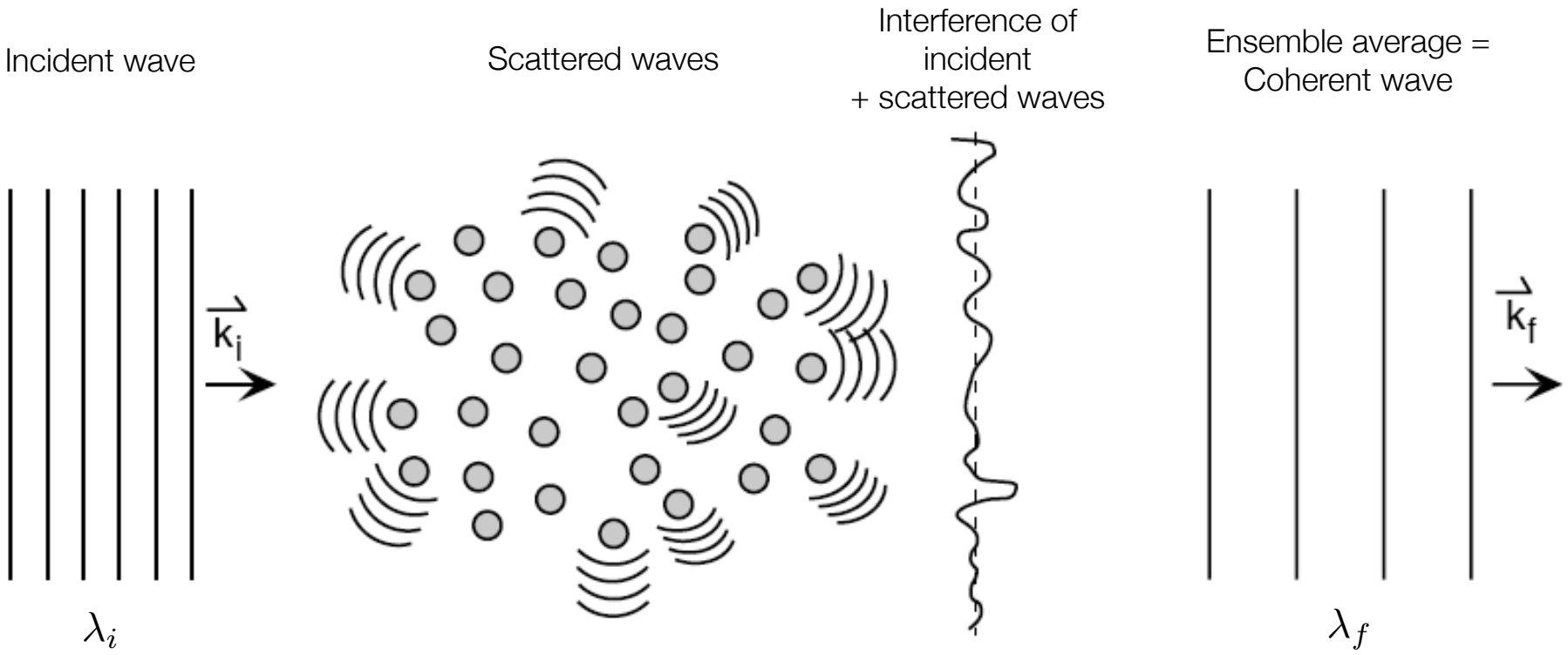

Example: index of refraction

$$n = \frac{c_{\mathrm{v}}}{c_{\mathrm{m}}} = \frac{\lambda_{\mathrm{v}}}{\lambda_{\mathrm{m}}}$$

air	water	glass	diamond
1,003	1,33	1,5	2,4

Introduction: wave propagation in disordered media

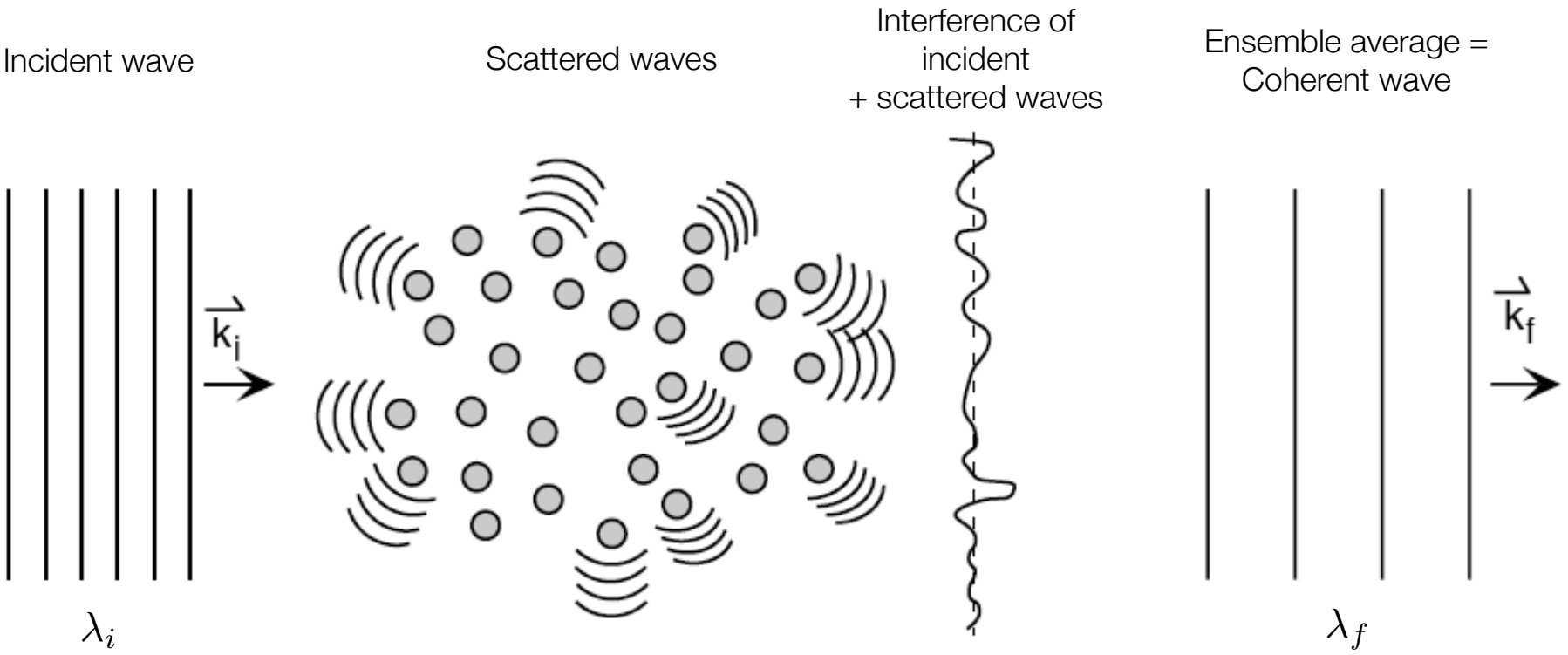

$$\psi_{\text{inc}} = \psi_o \bar{e}^{i(\omega t - kx)} \longrightarrow \psi_{\text{scatt}} \longrightarrow \psi = \psi_{\text{inc}} + \psi_{\text{scatt}} \longrightarrow \langle \psi \rangle$$

Introduction: wave propagation in disordered media

- Three transport modes:

  (1) Wave-like propagation (coherent wave)

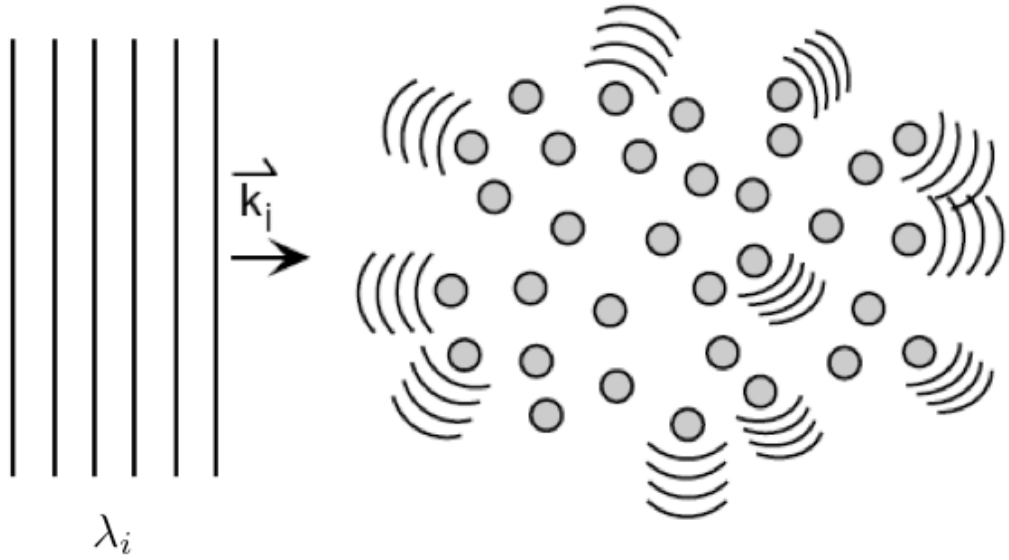

$\lambda \gg R$

Introduction: wave propagation in disordered media

- Three transport modes:

  (1) Wave-like propagation (coherent wave)

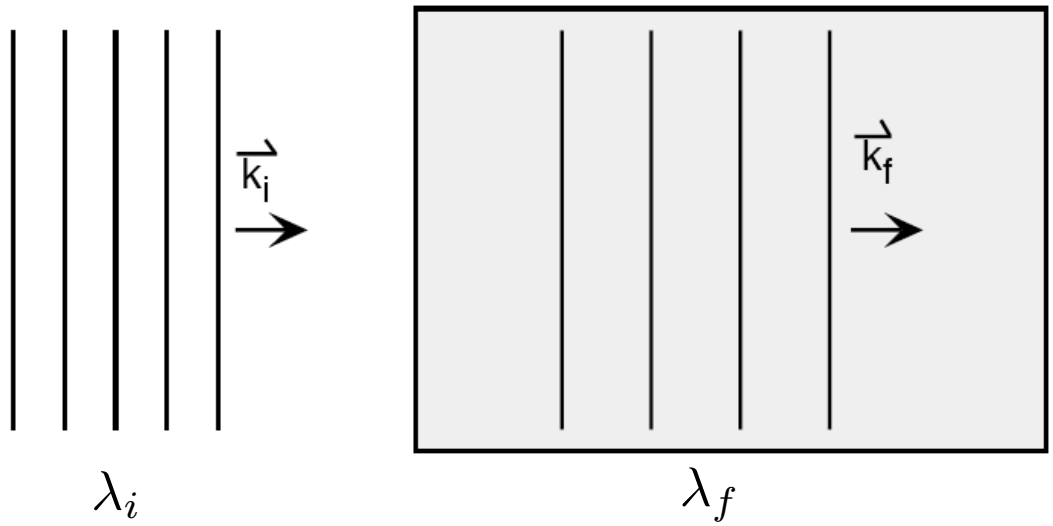

$$\lambda \gg R$$

$$\nabla^2 \langle \psi \rangle - \frac{1}{\tilde{c}_{\text{eff}}^2} \frac{\partial^2 \langle \psi \rangle}{\partial t^2} = 0$$

$\tilde{c}_{\text{eff}}$ is complex

Introduction: wave propagation in disordered media

- Three propagation modes:

  (1) Wave-like propagation (coherent wave)

$$\langle\psi\rangle \sim e^{-i\omega t} \qquad \nabla^2\langle\psi\rangle + \tilde{k}_{\text{eff}}^2\langle\psi\rangle = 0$$

$$\tilde{k}_{\text{eff}} = k_{\text{real}} + ik_{\text{imag}} \rightarrow \langle\psi\rangle \sim e^{i(\tilde{k}_{\text{eff}}x-\omega t)} \sim e^{i(k_{\text{real}}x-\omega t)}e^{-k_{\text{imag}}x}$$

Effective phase wave speed: $\rightarrow \quad c_{\text{eff}} \equiv \dfrac{\omega}{k_{\text{real}}}$

Effective absorption coefficient: $\rightarrow \quad \alpha_{\text{eff}} \equiv k_{\text{imag}}$

$$\alpha_{\text{eff}} = l_s^{-1} \quad \text{and} \quad l_s = \frac{1}{n\sigma_{\text{sc}}}$$ Scattering length scale

Introduction: wave propagation in disordered media

- Three propagation modes:

(2) Diffusive transport (incoherent wave)

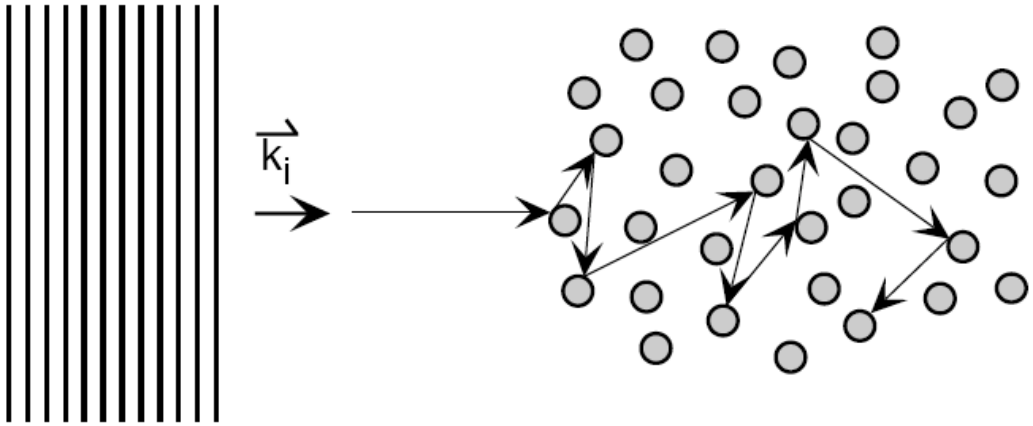

$$\lambda \ll R$$

Geometric ray propagation is like a random walk, which leads to diffusive transport

$$\frac{\partial \langle \psi^2 \rangle}{\partial t} = D \nabla^2 \langle \psi^2 \rangle$$

(3) Localization

$$D \to 0\ !$$

Example 1: blue and red sky

Why blue?

Example 1: blue and red sky

Why blue?

Why clouds are white?

Example 1: blue and red sky

Why red?

Example 1: blue and red sky

Scattering length scale

$$l_s = \frac{1}{n\sigma_{\rm sc}}$$

Rayleigh Scattering for $\lambda \gg R$

$$\begin{aligned} \sigma_{\rm sc} &\sim R^6\omega^4 \\ l_s &\sim \omega^{-4} \end{aligned}$$

Blue light is scattered more efficiently

Red light attenuated less efficiently

Example 1: blue and red sky

Scattering length scale

$$l_s = \frac{1}{n\sigma_{\rm sc}}$$

Rayleigh Scattering for $\lambda \gg R$

$$\begin{aligned} \sigma_{\rm sc} &\sim R^6\omega^4 \\ l_s &\sim \omega^{-4} \end{aligned}$$

Blue light is scattered more efficiently

Red light attenuated less efficiently

Example 1: blue and red sky

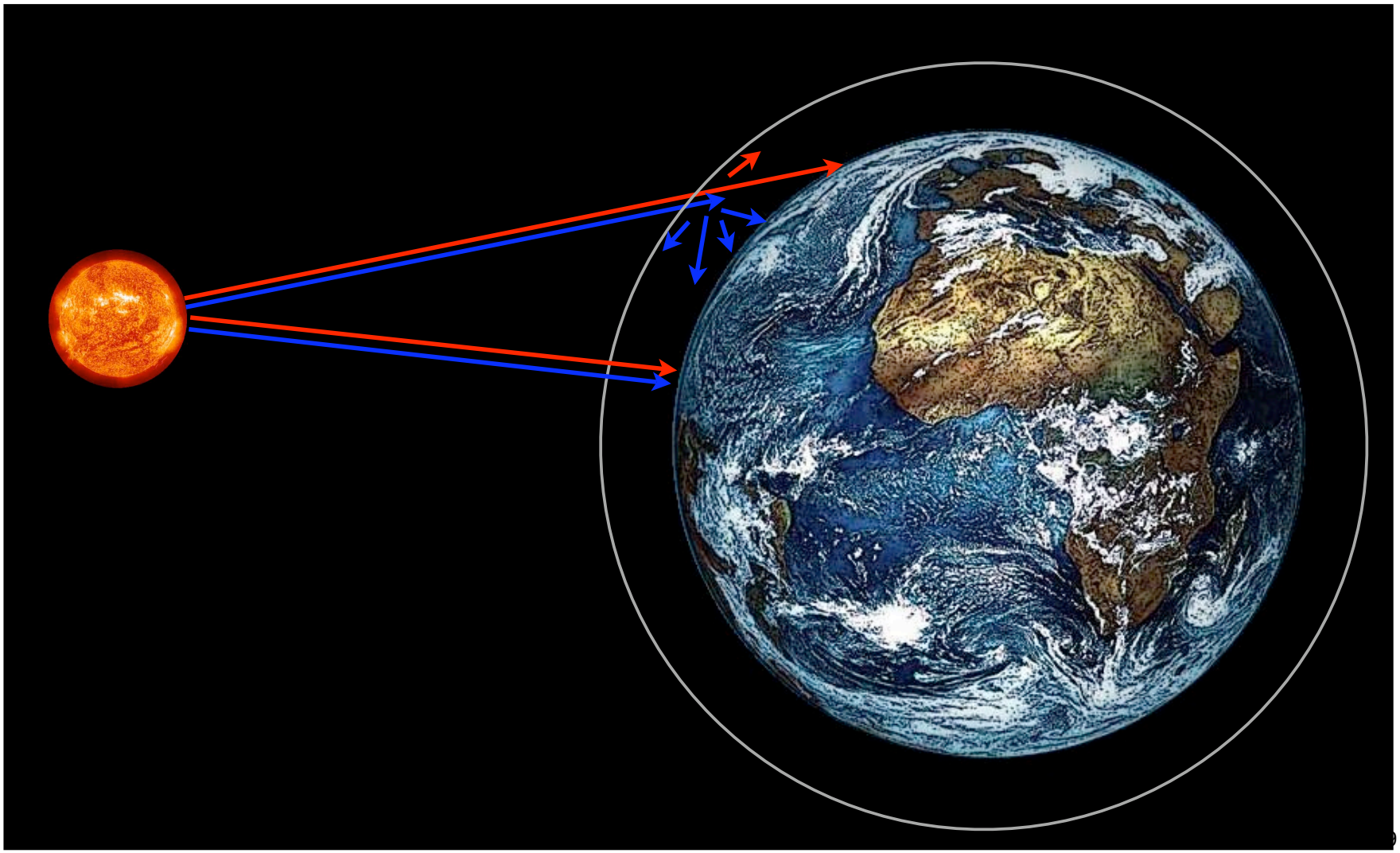

Example 2: sound in bubbly liquids

- Wijngaarden-Papanicolaou Model: low volume fraction

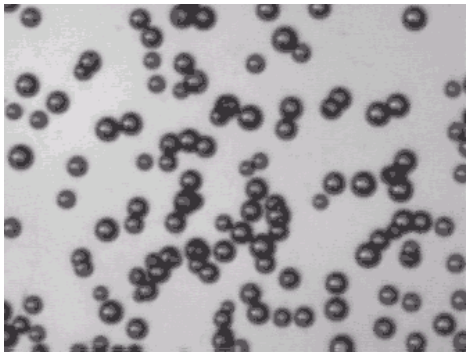

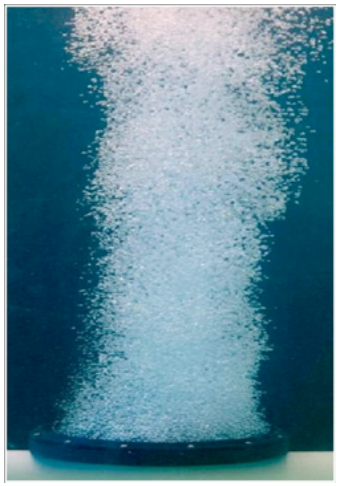

$$
\begin{aligned}
c_{\text{eff}}^2 &= \frac{1}{\langle\rho\rangle\langle\chi\rangle} \\
\langle\rho\rangle &= \rho_g\phi + \rho_l(1-\phi) \\
\langle\chi\rangle &= \chi_g\phi + \chi_l(1-\phi)
\end{aligned}
$$

$$\rho_l \gg \rho_g \qquad \& \qquad \chi_l \ll \chi_g$$

$$\boxed{c_{\text{eff}}^2 \approx \frac{1}{\rho_l\chi_g(1-\phi)\phi}} \qquad \chi_g = \frac{1}{\gamma P_o}$$

Wood's formula ($c_{\text{w}} \equiv c_{\text{eff}}$)

Example 2: sound in bubbly liquids

- Effective velocity

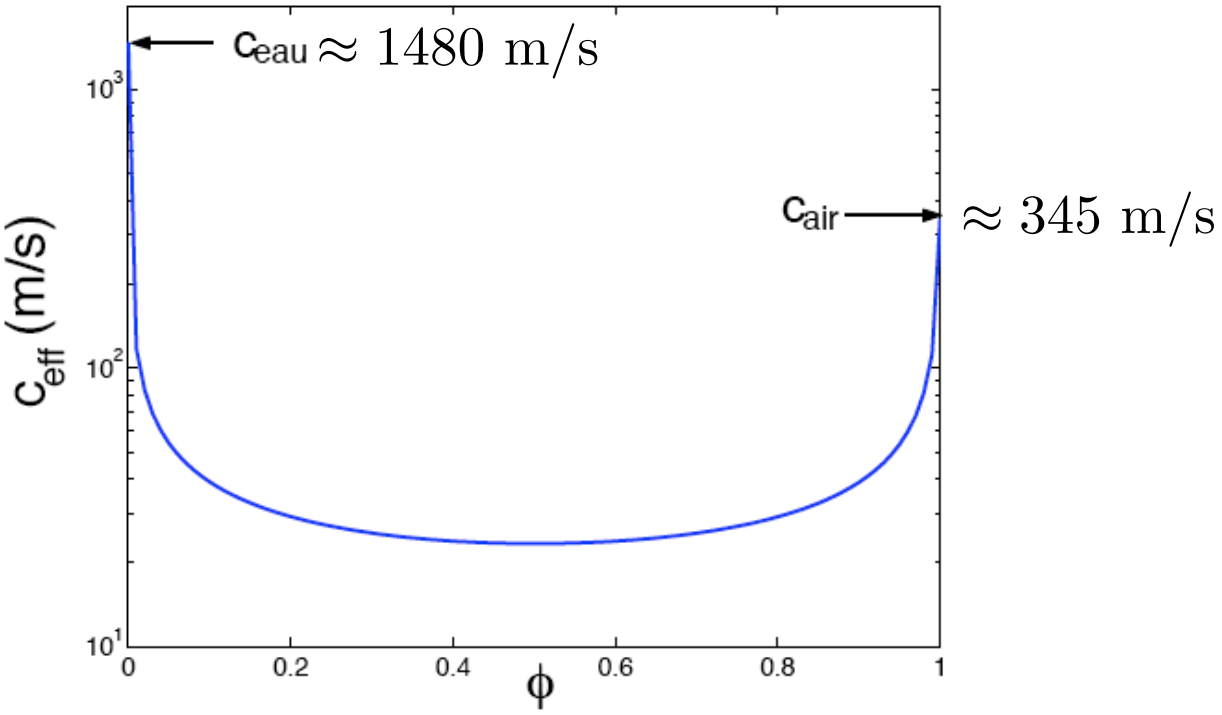

$$\rho_l \gg \rho_g \qquad \& \qquad \chi_l \ll \chi_g$$

Example 2: sound in bubbly liquids

- Effective velocity

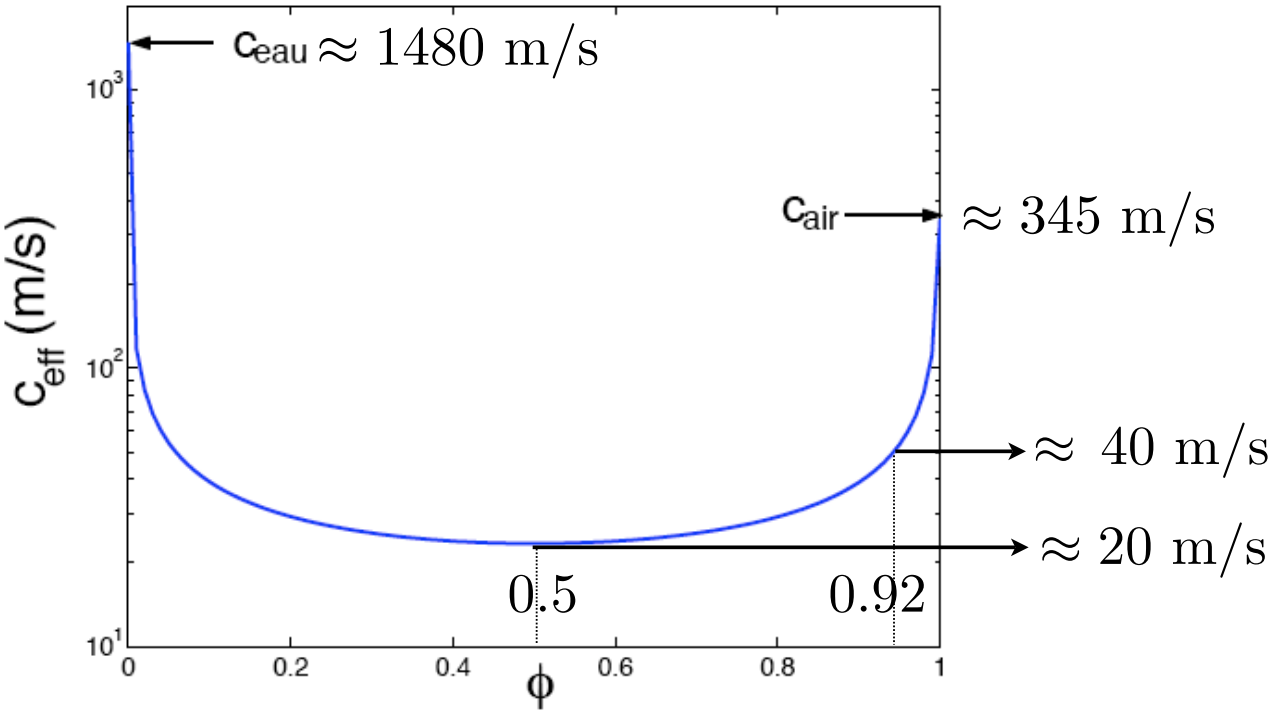

$\rho_l \gg \rho_g \quad \& \quad \chi_l \ll \chi_g$

Example 2: sound in bubbly liquids

- Effective velocity

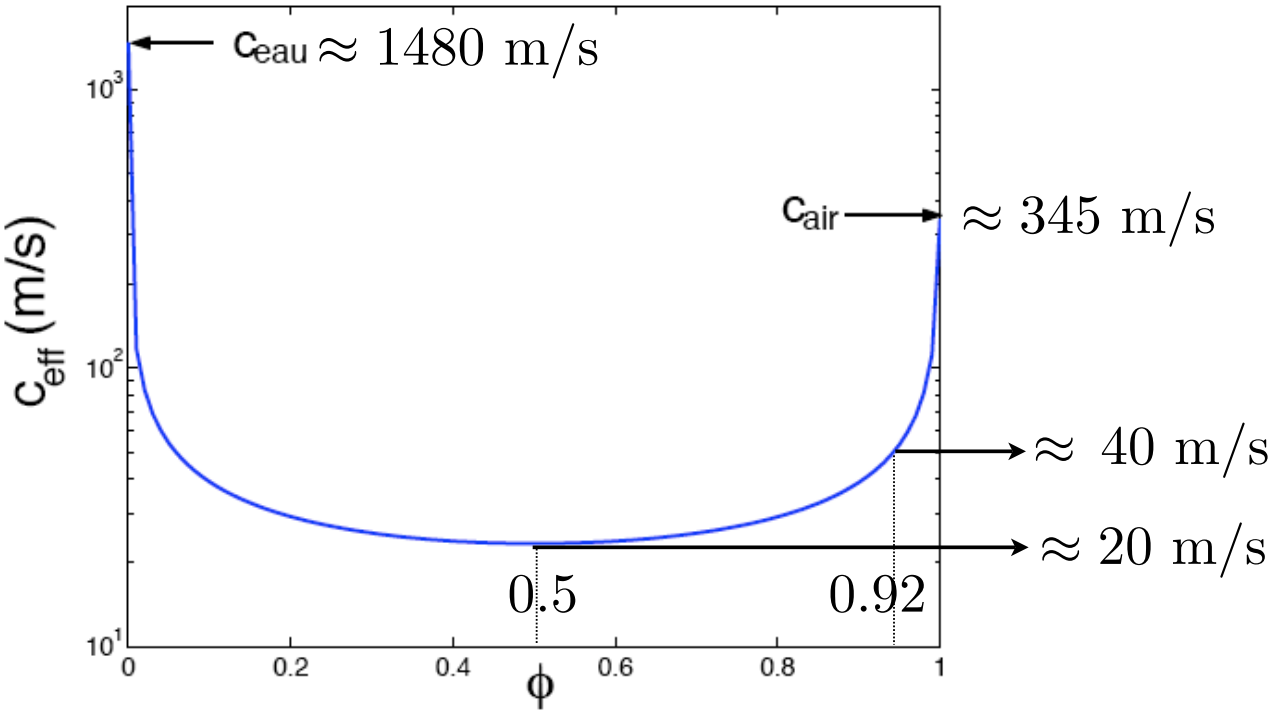

$\rho_l \gg \rho_g \quad \& \quad \chi_l \ll \chi_g$

Very low velocity compared to pure liquid and gas!

Example 2: sound in bubbly liquids

- Effective absorption

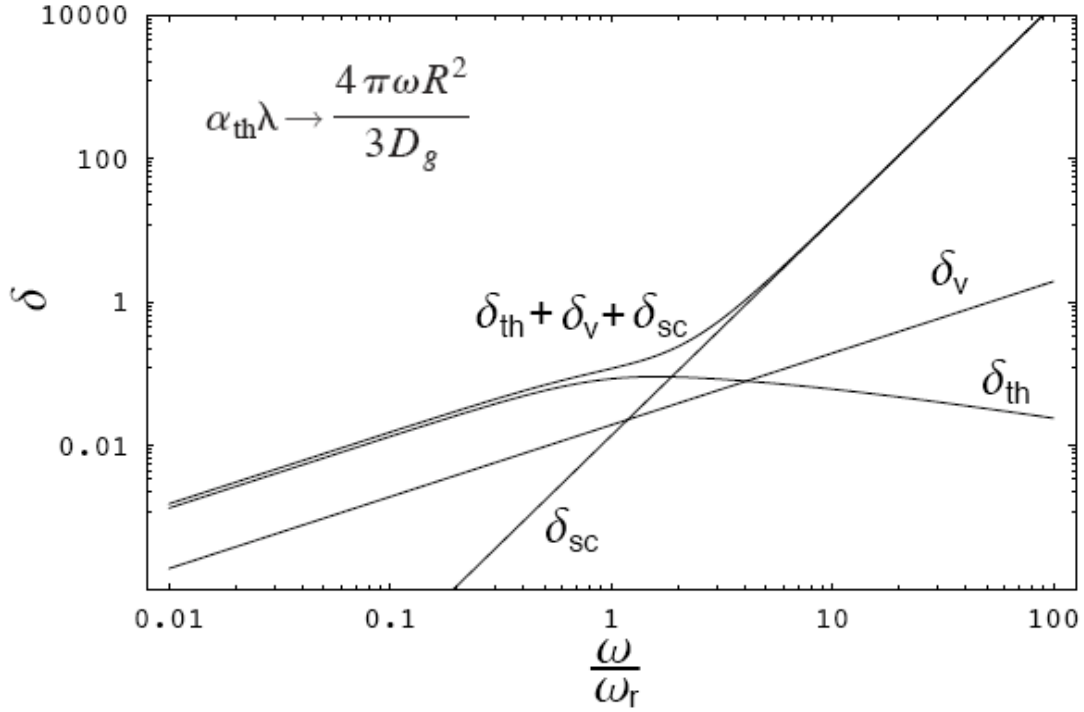

$$\Pi^t_{\text{wall}} \propto (T_{\text{ac}}/l_t)^2 \gg \Pi^t_{\text{vol}} \propto (T_{\text{ac}}/\lambda)^2$$

Example 2: sound in bubbly liquids

- Effective absorption

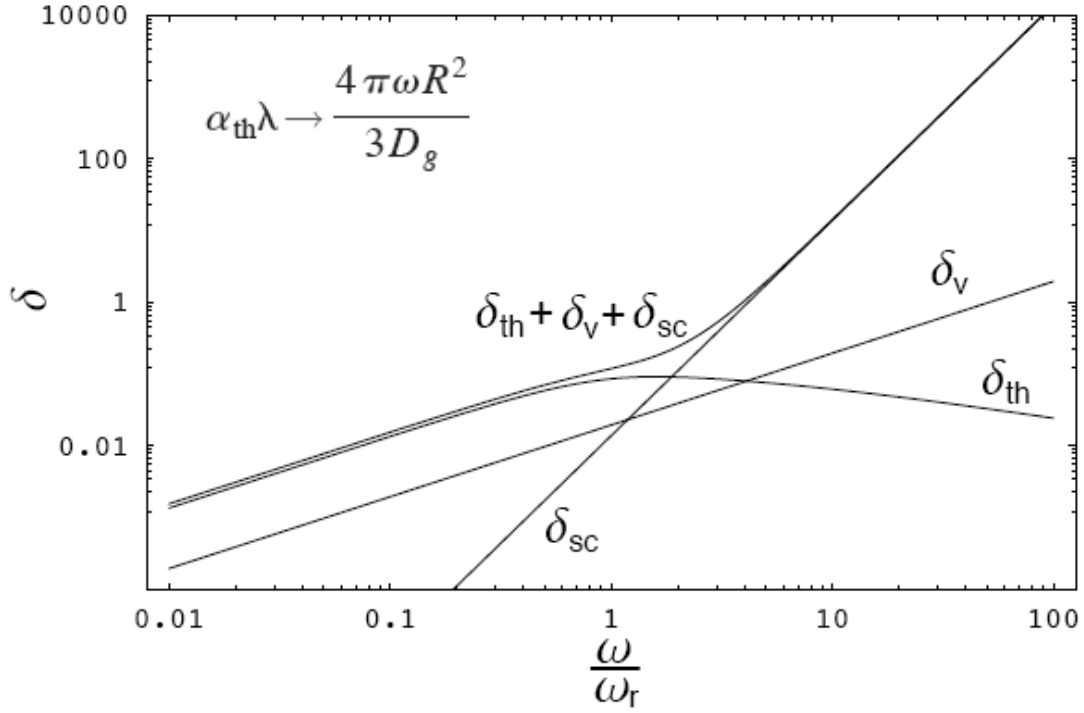

$$\Pi^t_{wall} \propto (T_{ac}/l_t)^2 \gg \Pi^t_{vol} \propto (T_{ac}/\lambda)^2$$

Very high absorption compared to pure liquid and gas!

Part 1: Coarsening of shaving foam (pulse propagation technique)

"Gillette Regular" shaving foam $\phi = \frac{V_g}{V_t} \approx 0.92$ $\langle R \rangle \approx 15\,\mu\mathrm{m}$

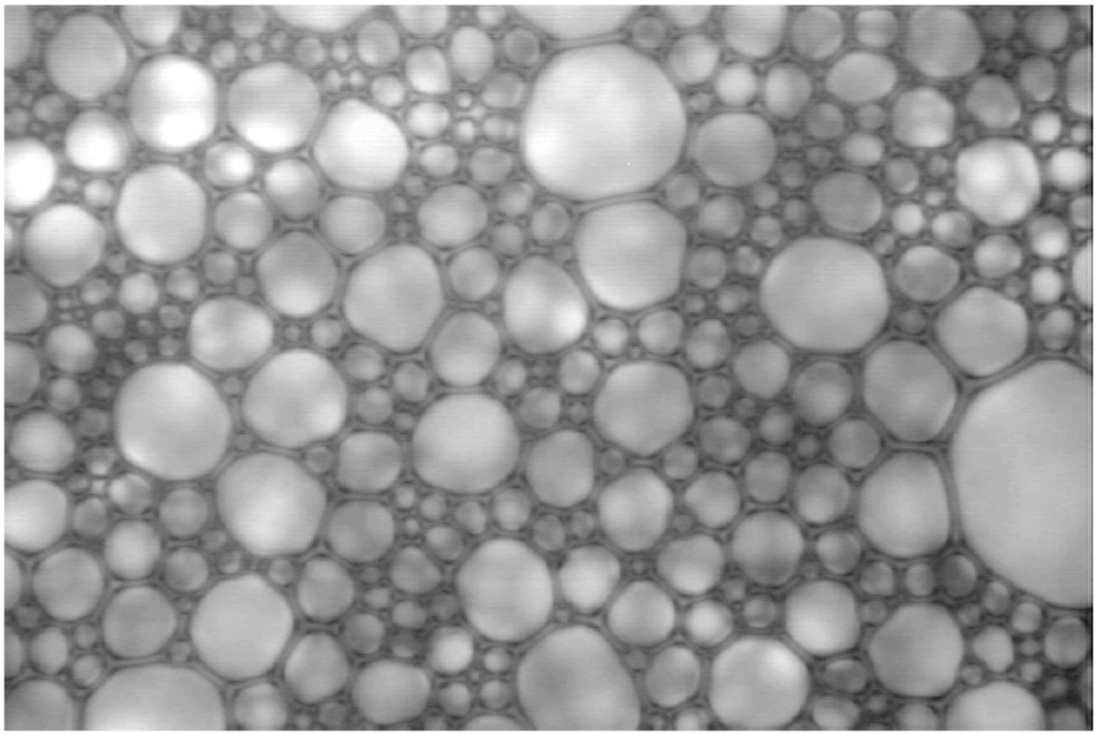

Collection of highly compacted gas bubbles embedded in a liquid matrix

With Stéphan Fauve from LPS-ENS Paris

Shaving foam: Multiple scale system

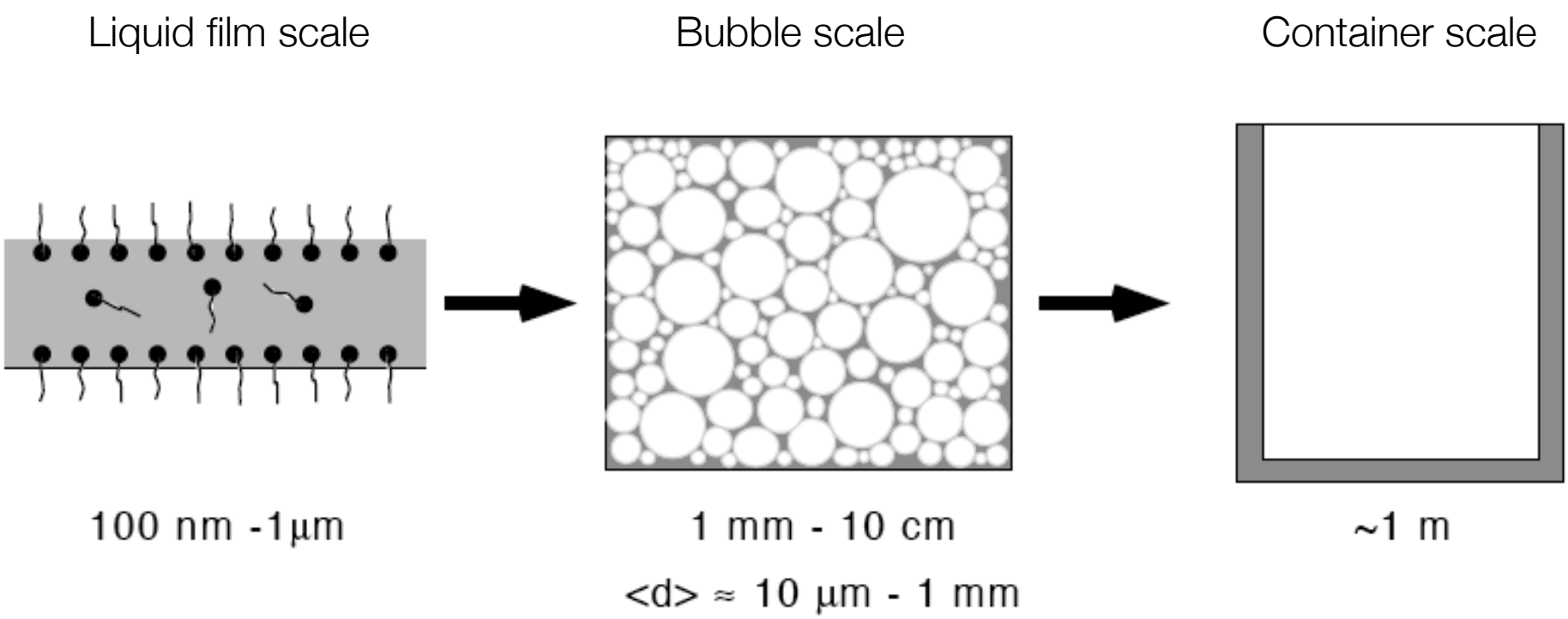

These scales are coupled in nontrivial ways

Foam structure: bubble size distribution

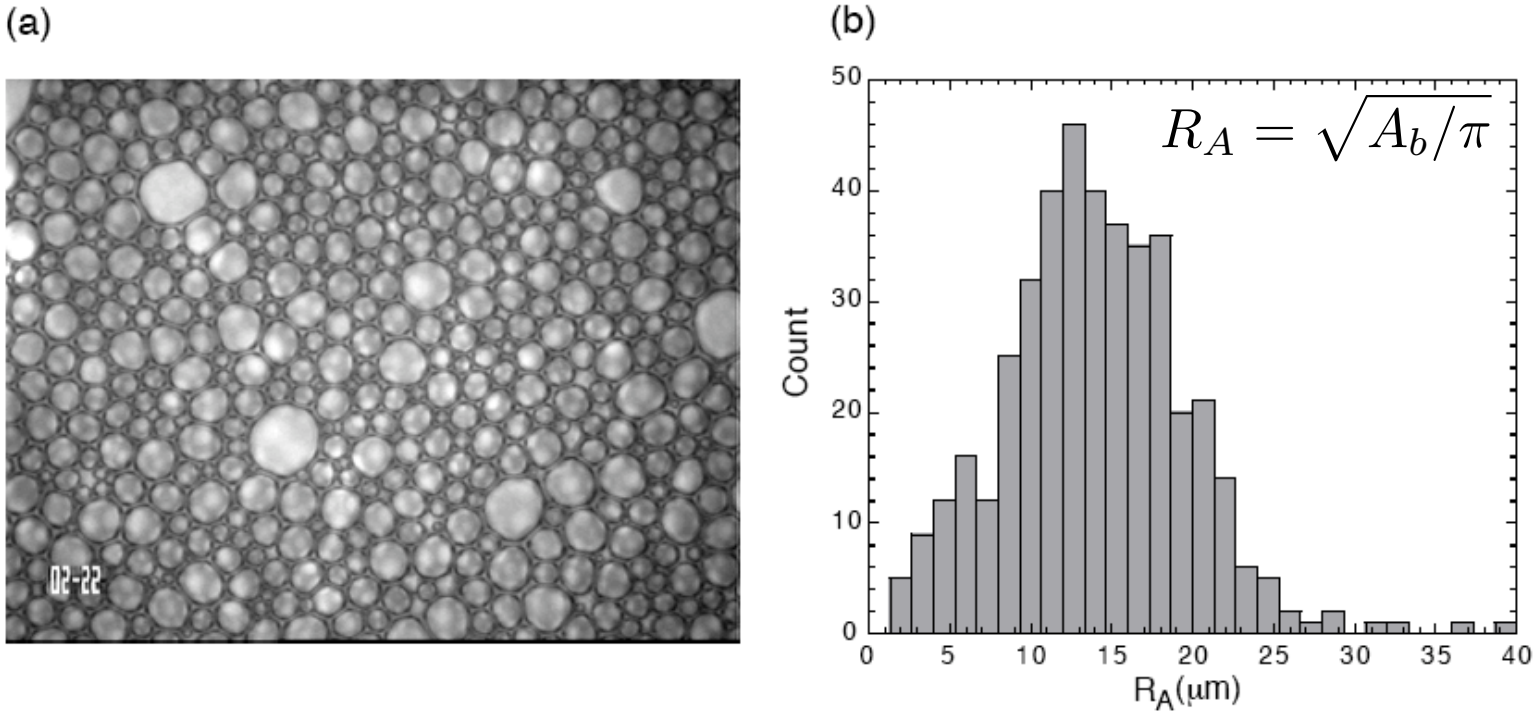

FIG. 2.3 – *(a) Image microscopique d'une mousse à raser. Le rayon moyen est* $\langle R_A \rangle \approx 14 \pm 5.5$ *μm et la fraction volumique du gaz est* $\phi \approx 0.92$. *(b) Histogramme de* R_A, *le nombre total de bulles est* 420.

Coarsening foam: aging mechanisms

- Foams are never in equilibrium, their structure evolves in time...
- There are three aging mechanisms:

  (1) Liquid drainage due to gravity (bears, sodas)

  (2) Bubble coalescence due to film rupture (water-soap foam)

  (3) Gas diffusion between neighbor bubbles due to Laplace pressure difference (from small to large bubbles through liquid film)

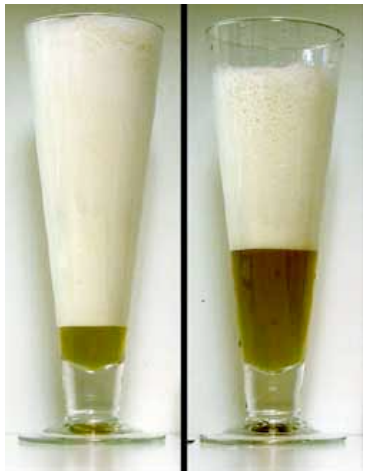

$\langle R \rangle \approx 1\,\mathrm{mm}$

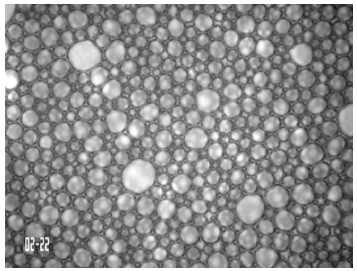

$\langle R \rangle \approx 10\,\mu\mathrm{m}$

Aging shaving foam: drainage effect

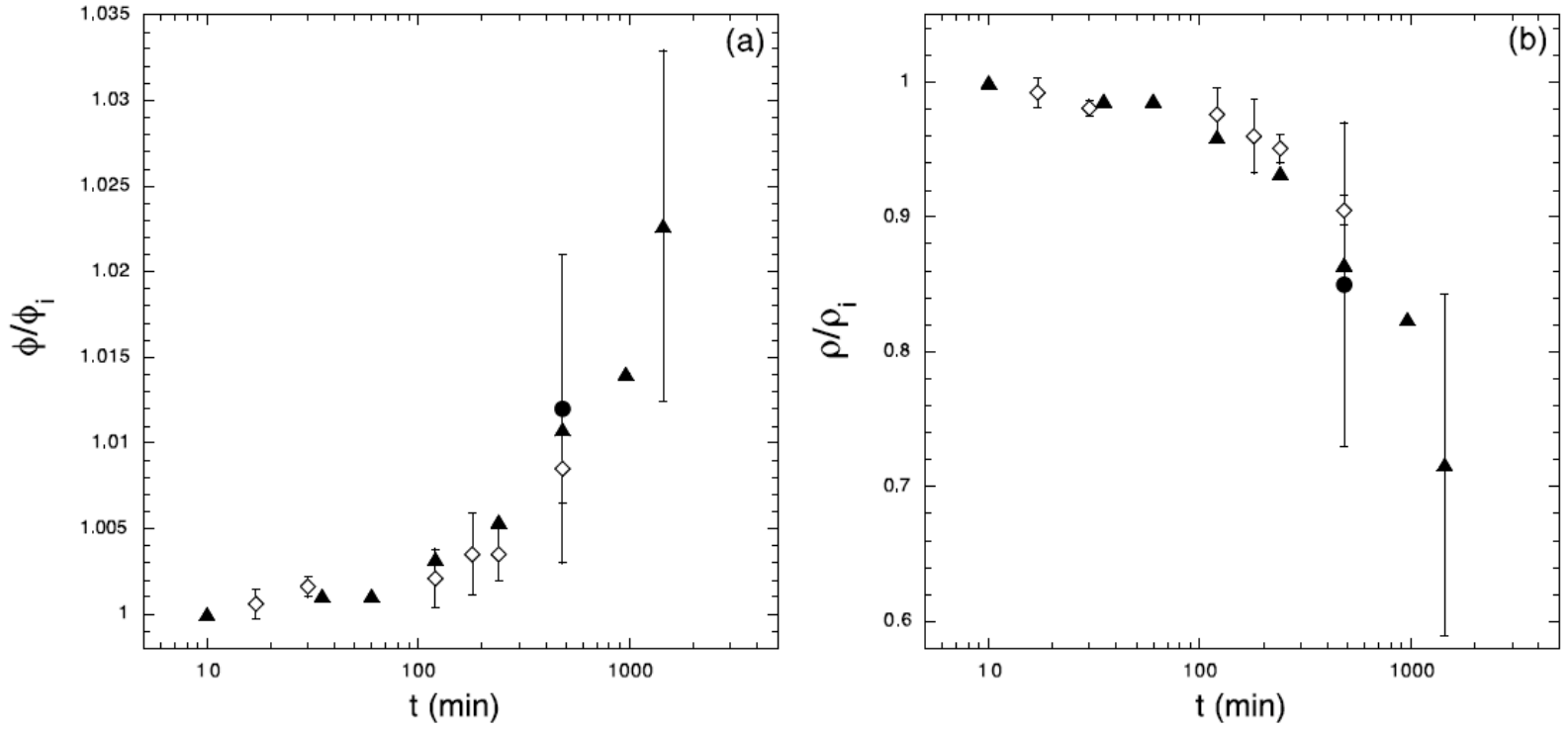

FIG. 2.7 – *Évolution temporelle de la fraction volumique de gaz (a) et de la densité (b) pour les deux dispositifs expérimentaux ; (●) dispositif I, (◇) dispositif II. Nous présentons aussi les données obtenues par Hoballah et al [48] (▲). Toutes les données sont normalisées par rapport aux valeurs initiales.*

Coarsening foam: aging mechanisms

- When gas diffusion is dominant, foam structure evolves in a self-similar way. This means that the structure is slave of the evolution of a single length, like the average radius <R(t)>.

- For Shaving Foams, it has been shown that

$$\langle R(t)\rangle^2 - \langle R(t_o)\rangle^2 = A(t - t_o).$$

- <R(t)> ≈ 15, 30 and 50 μm for t = 20, 120 and 480 min

Can we probe foam structure evolution with acoustics?

Can we probe foam structure evolution with acoustics?

Orenbakh & Shushkov, Acoust. Phys., vol. 39, 63 (1993)

$$\phi \approx 0.95 \;\rightarrow\; c_l \approx 50 \text{ m/s} \qquad (c_\text{w} \approx 49.8 \text{ m/s})$$

Q. Sun, J.P. Butler, B. Suki, & D. Stamenovic, J. Coll. Int. Sci., vol. 163, 269 (1994)

$$c_t \approx 3 \text{ m/s} \qquad \left(c_\text{shear} \approx \sqrt{\frac{2\sigma}{\langle R \rangle \langle \rho \rangle}} \approx 6 \text{ m/s} \right)$$

N. Mujica & S. Fauve, Phys. Rev. E, vol. 66, 021404 (2002)

$$\phi \approx 0.92 \;\rightarrow\; c_l \approx 65 - 45 \text{ m/s} \qquad (c_\text{w} \approx 40 \text{ m/s})$$

Sound speed and absorption coefficient

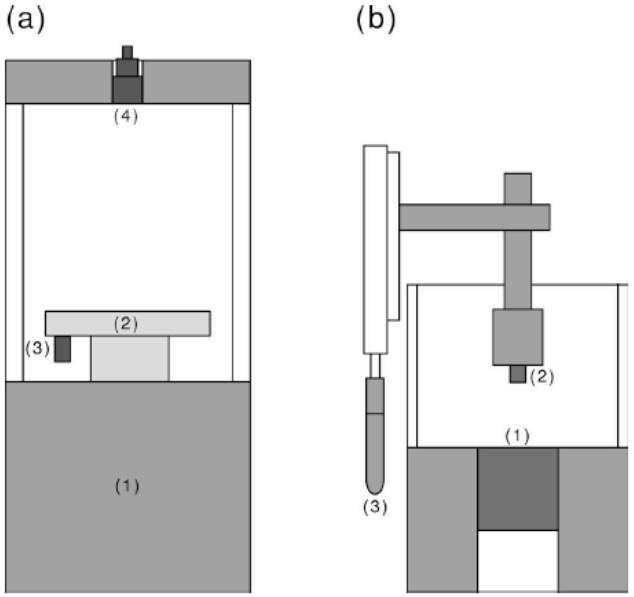

FIG. 1. Sketches of the experimental apparatus. (a) Low acoustic frequencies: (1) electromechanical vibration exciter, (2) piston, (3) piezoelectric accelerometer, and (4) pressure sensor. (b) High acoustic frequencies: (1) acoustic transducer, (2) pressure sensor, and (3) micrometer displacement controller.

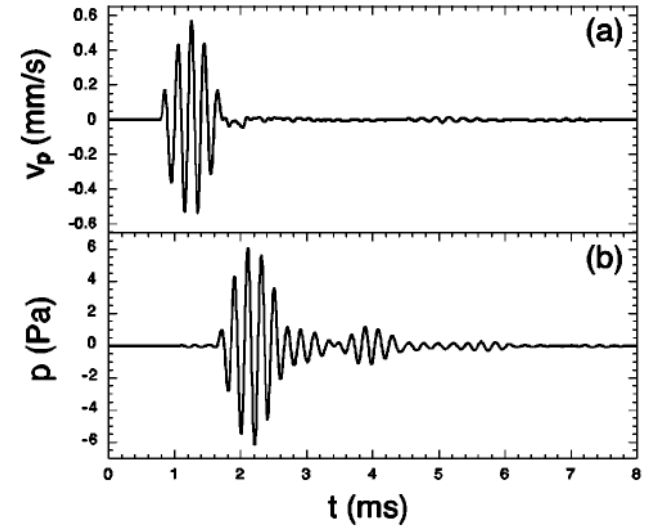

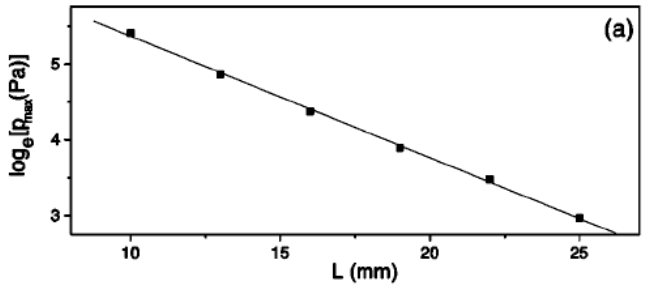

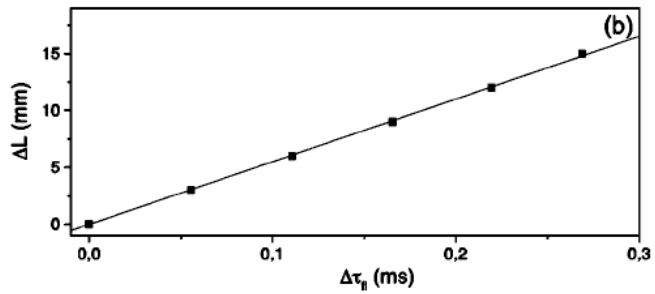

$$f = 5 \text{ kHz}$$
$$L = 56 \text{ mm}$$
$$c \approx 65 \text{ m/s}$$

$$f = 37 \text{ kHz}$$
$$\lambda \approx 1.5 \text{ mm}$$
$$1/\alpha \approx 6.3 \text{ mm}$$
$$\alpha\lambda \approx 0.24$$

Foam sample reproducibility: average density depends on can age...

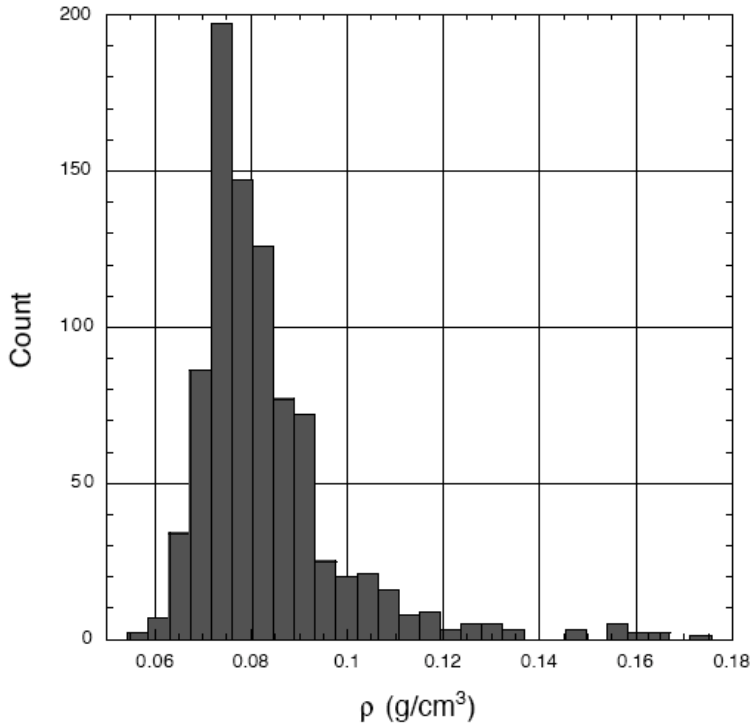

FIG. 2.8 – *Histogramme de $\langle\rho\rangle$ pour des échantillons relativement «jeunes» de mousse, où le drainage du liquide n'a pas encore affecté la densité du système (temps de vieillissement $<$ 60 min). Le nombre total de mesures est 875. 72% des valeurs mesurées se trouvent dans la gamme $\langle\rho\rangle = 0.067 - 0.089$ g/cm^3. Les mesures $\langle\rho\rangle \gtrsim 0.09$ g/cm^3 correspondent à des échantillons fabriqués soit au tout début soit à la fin de la «vie utile» d'une bonbonne de mousse.*

Foam sample reproducibility: Foam structure depends on how you press the button...

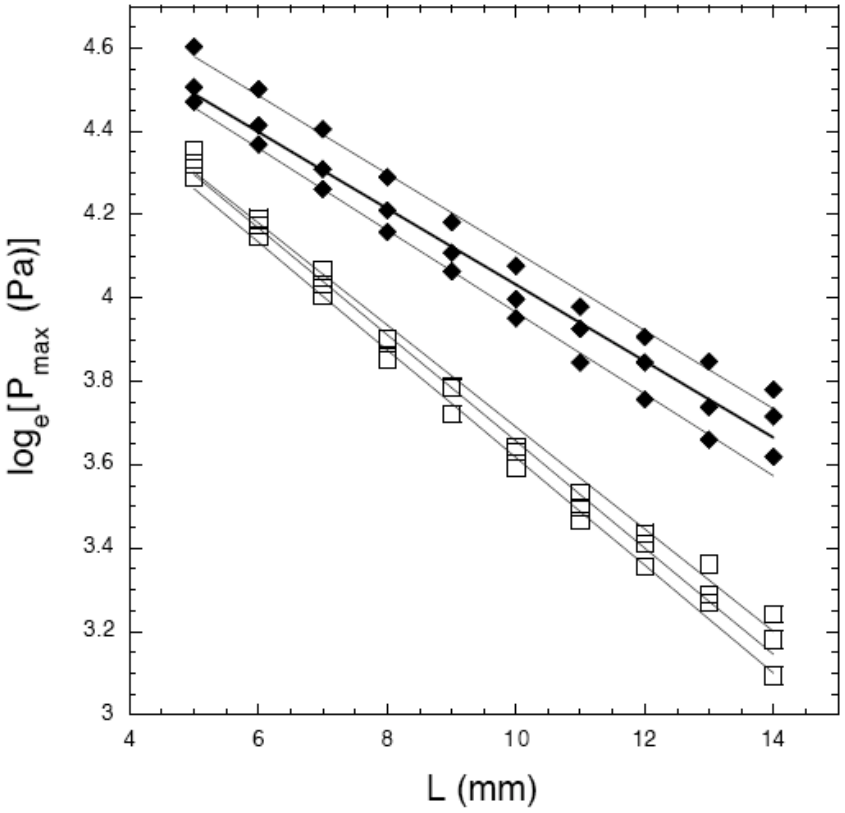

FIG. 2.9 – *Effet de la «vitesse» de fabrication d'une mousse sur l'atténuation pour une densité constante* $\langle\rho\rangle = 0.076 \pm 0.005$. (□) *fabrication «lente»*, $\alpha = 128.1$, 129.2 *et* 122.5 *1/m ;* (♦) *fabrication «rapide»*, $\alpha = 91.8$, 98.2 *et* 94.1 *1/m.*

Foam sample reproducibility: results and ensemble average

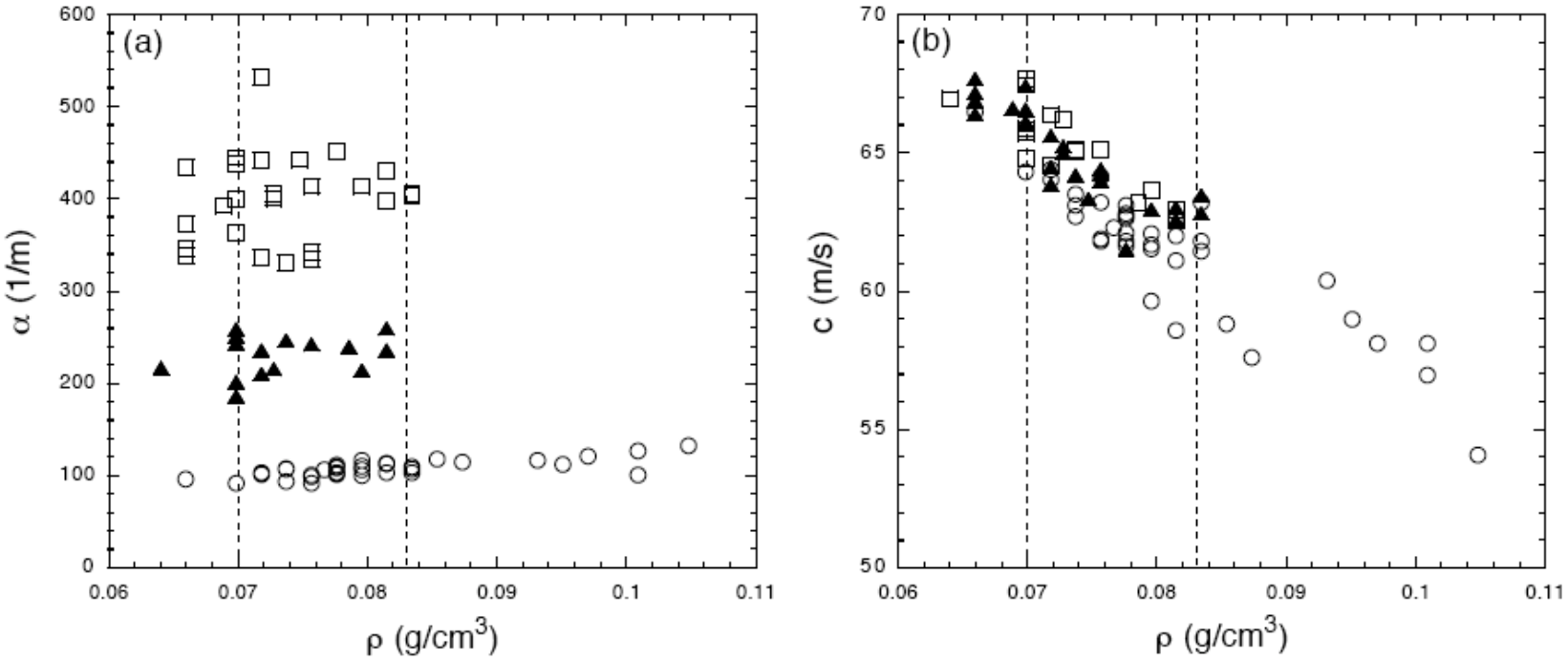

FIG. 2.10 – *Reproductibilité des mesures : α et c en fonction de la densité pour $f = 37$ ($\circ$), 63 ($\blacktriangle$) et 84 ($\square$) kHz. Les mesures ont été réalisées 5 min après la formation de la mousse. Les lignes verticales indiquent la gamme de densité $\langle\rho\rangle = 0.070 - 0.083$ g/cm^3 considérée pour les moyennes d'ensemble.*

Foam aging

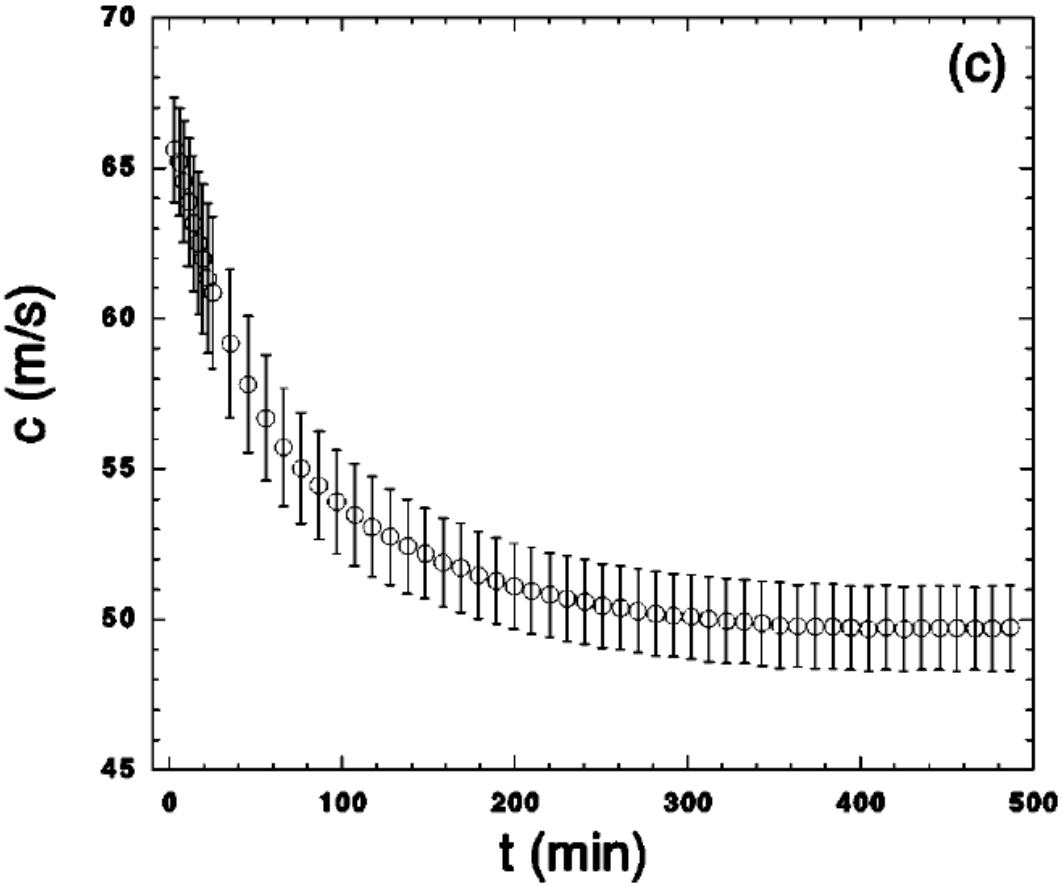

$$f = 5 \text{ kHz}, \quad \langle \rho \rangle = 0.076 \pm 0.005 \text{ g/cm}^3$$

Foam aging

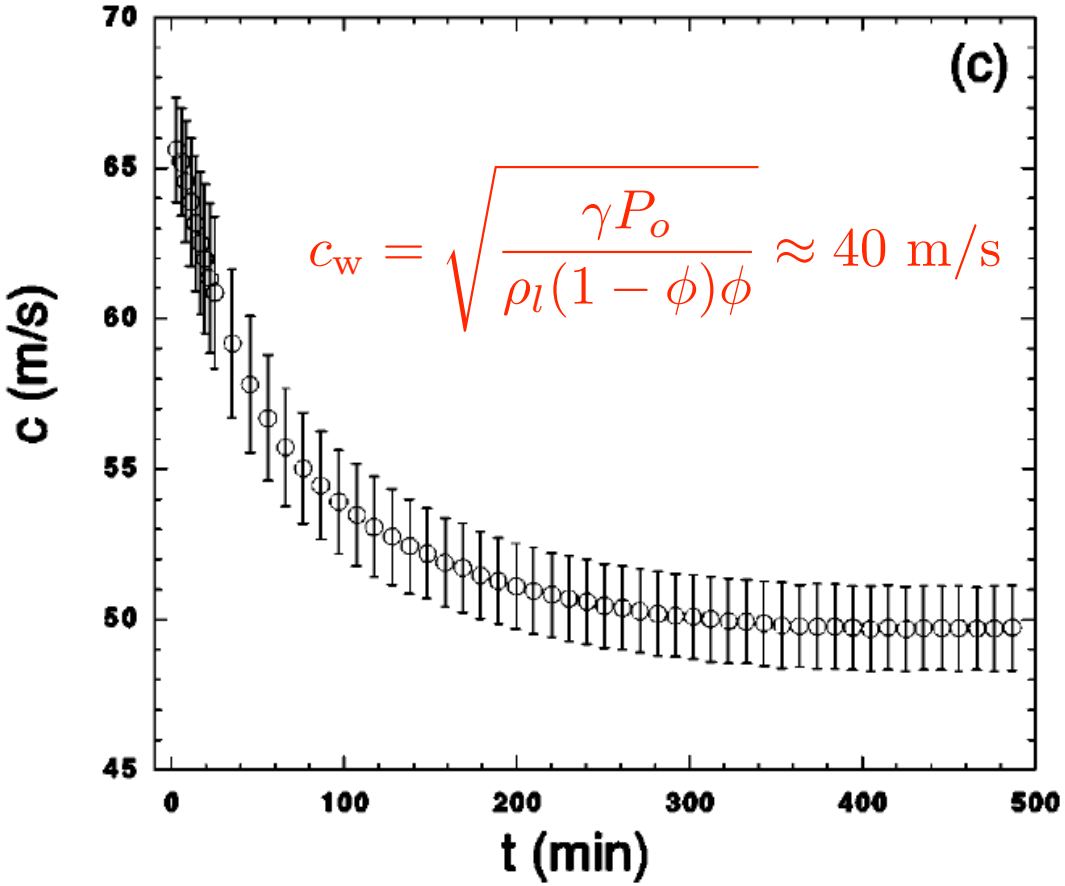

$$c_{\mathrm{w}} = \sqrt{\frac{\gamma P_o}{\rho_l (1-\phi)\phi}} \approx 40 \text{ m/s}$$

$$f = 5 \text{ kHz}, \quad \langle \rho \rangle = 0.076 \pm 0.005 \text{ g/cm}^3$$

Foam aging

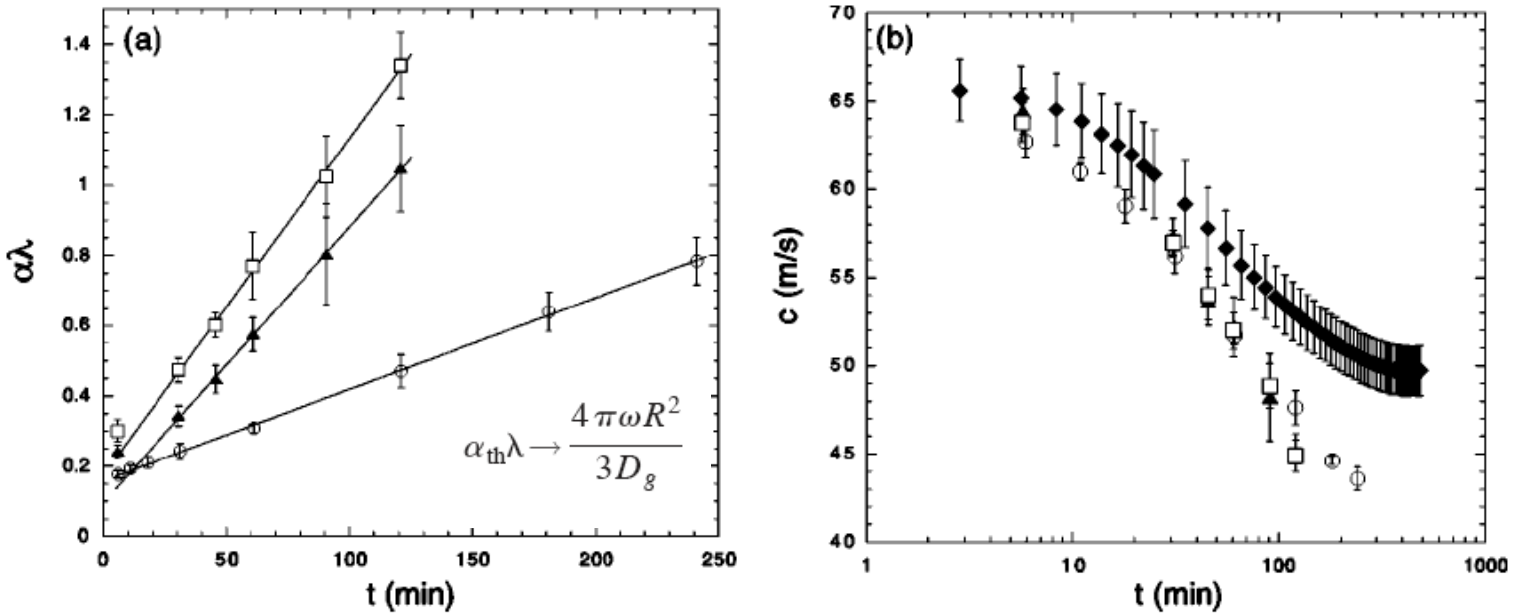

FIG. 5. (a) Time evolution of $\alpha\lambda$ for $f=37$ (○), 63 (▲), and 84 (□) kHz. The continuous lines correspond to linear fits $\alpha\lambda = a + bt$ for $t > 20$ min. The parameters are $a=0.159$, 0.097, and 0.175, $b=2.61\times10^{-3}$, 7.84×10^{-3}, and 9.58×10^{-3} min^{-1}, respectively. The linear regression coefficients are $R_c=0.9996$, 0.9998, and 0.9992, respectively. (b) Time evolution of c, in linear-$\log_{10}$ scale, for $f=5$ (◆), 37 (○), 63 (▲), and 84 (□) kHz. The ensemble-averaged density is $\langle\rho\rangle = 0.076 \pm 0.005$ g/cm^3.

Higher velocity and age time dependence?

- Foam film elasticity

Normal fluid film

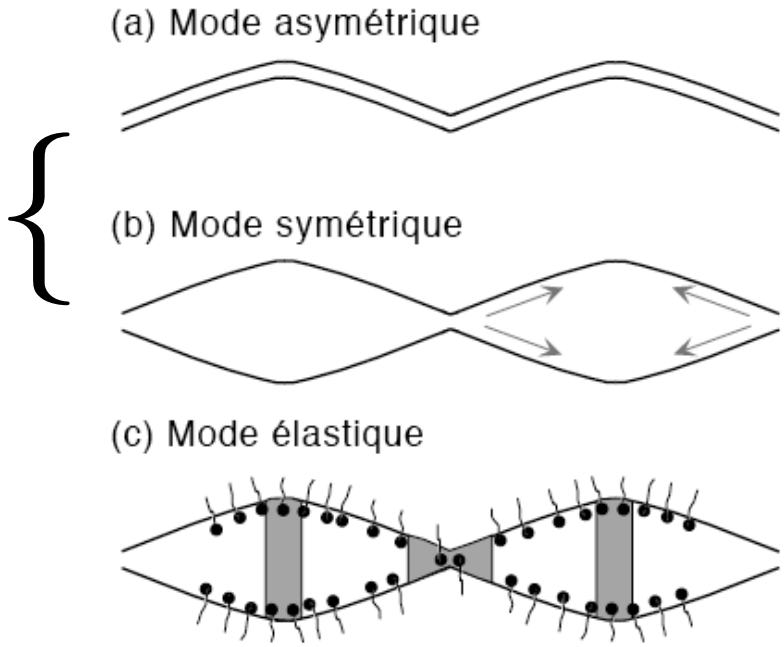

Soap film

Slow deformations: Gibbs elasticity
Fast deformations: Marangoni elasticity

Higher velocity and age time dependence?

- Foam film elasticity

Normal fluid film

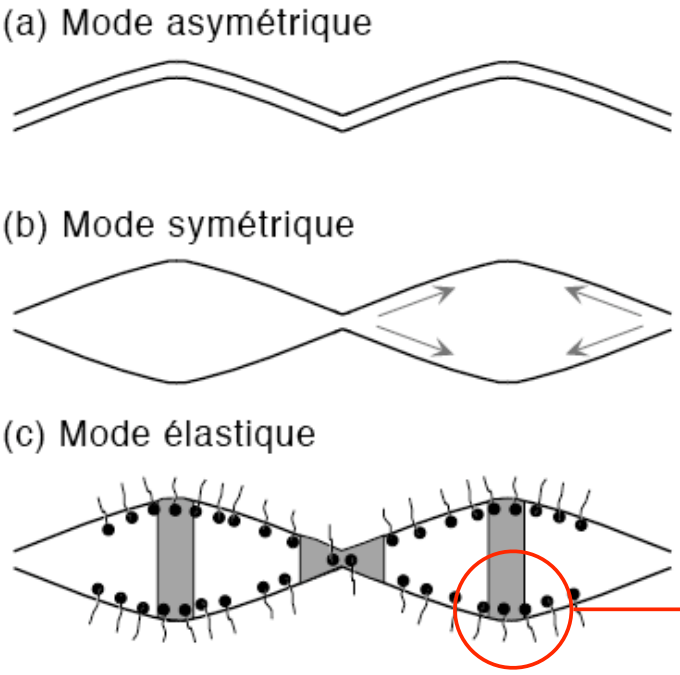

Soap film

surfactant concentration decreases, surface tension increases

Slow deformations: Gibbs elasticity
Fast deformations: Marangoni elasticity

Higher velocity and age time dependence?

- Foam film elasticity + Biot theory for sound propagation in porous media

Liquid skeleton has rigidity K_b

$$c_l^2 = \frac{1 + \phi\chi_g K_b}{\langle\rho\rangle\phi\chi_g} \;\; ; \;\; c_t^2 = \frac{\mu}{\langle\rho\rangle}$$

$$K_b \approx \frac{2E_M}{h} \qquad \phi \approx \frac{\langle R(t)\rangle^3}{\langle R(t) + h(t)/2\rangle^3} \qquad \langle h(t)\rangle = B\langle R(t)\rangle$$

$$K_b \approx \frac{2E_M}{B\langle R(t)\rangle}$$

Higher velocity and age time dependence?

- Foam film elasticity + Biot theory for sound propagation in porous media

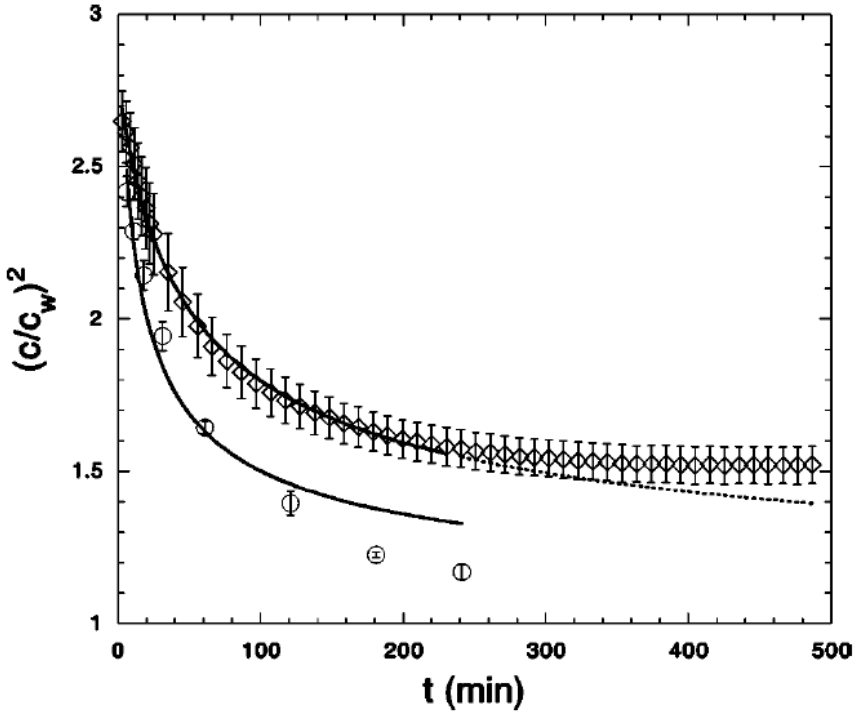

FIG. 7. Time evolution of $(c/c_w)^2$ for $f=5$ ($\diamond$) and 37 ($\bigcirc$) kHz. The continuous lines correspond to fits of the form $[c(t)/c_w]^2=1+a/\sqrt{1+b(t-t_o)}$ for $t<240$ min (see Table I for the values of a and b). The dashed line shows the extrapolation of the fit for $f=5$ kHz.

$$\left(\frac{c_1(t)}{c_w}\right)^2 = 1+\frac{a}{\sqrt{1+b(t-t_o)}}$$

$$a=\frac{2\phi E_M}{B\gamma P_o\langle R_o\rangle},$$

$$b=\frac{A}{\langle R_o\rangle^2}.$$

$$E_M \approx 60 \text{ mN/m}$$

Summary part 1

- Sound speed and absorption can be probed non-invasively and they both depend on foam structure

- Thermal conduction dominates attenuation

- (1) High sound speed compared to Wood's formula and (2) its evolution with age time are both attributed to the foam's liquid skeleton elasticity governed by Marangoni Elasticity

Hands on session: Coarsening shaving foam

- Simple acoustic setup

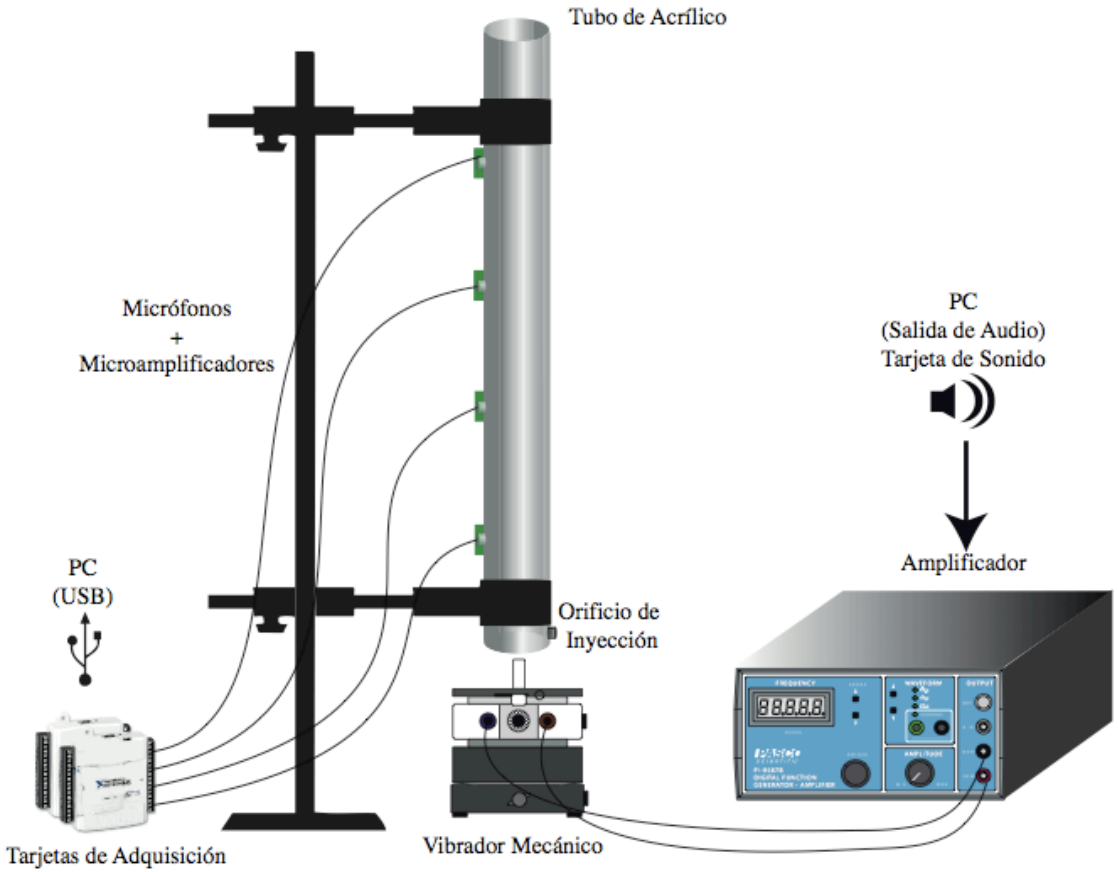

Electret Microphone

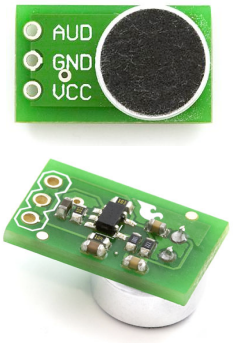

8 usd @
www.sparkfun.com

$L \approx 30$ cm $\quad D \approx 4$ cm $\quad f = 1$ kHz $\quad \lambda \approx 5$ cm

“Hands on foam session”

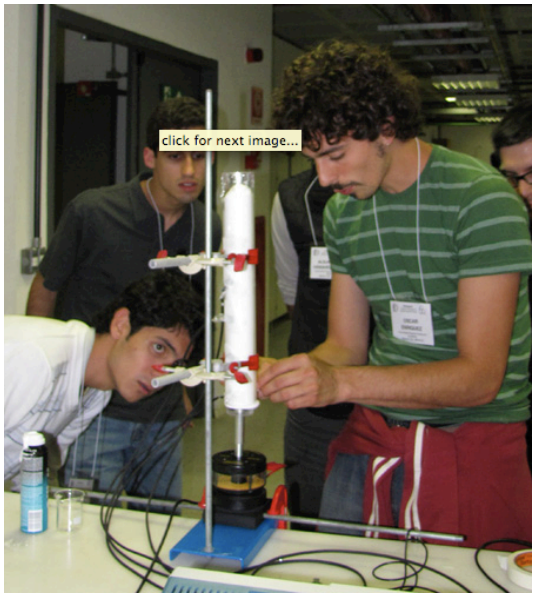

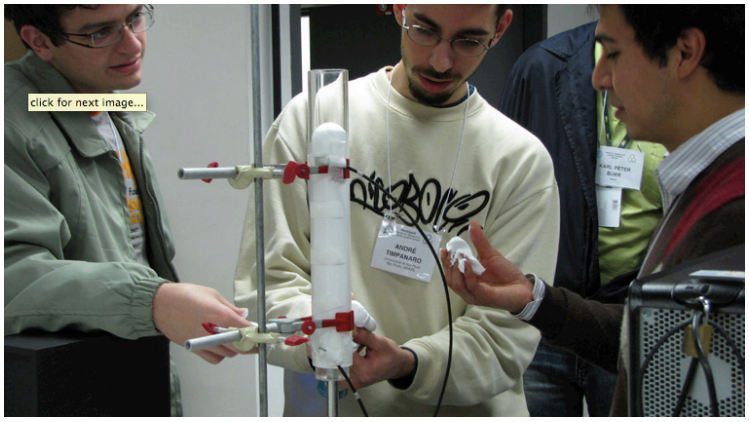

Thanks to Beth for pics

Hands on session: Coarsening shaving foam

- Results from hands on session

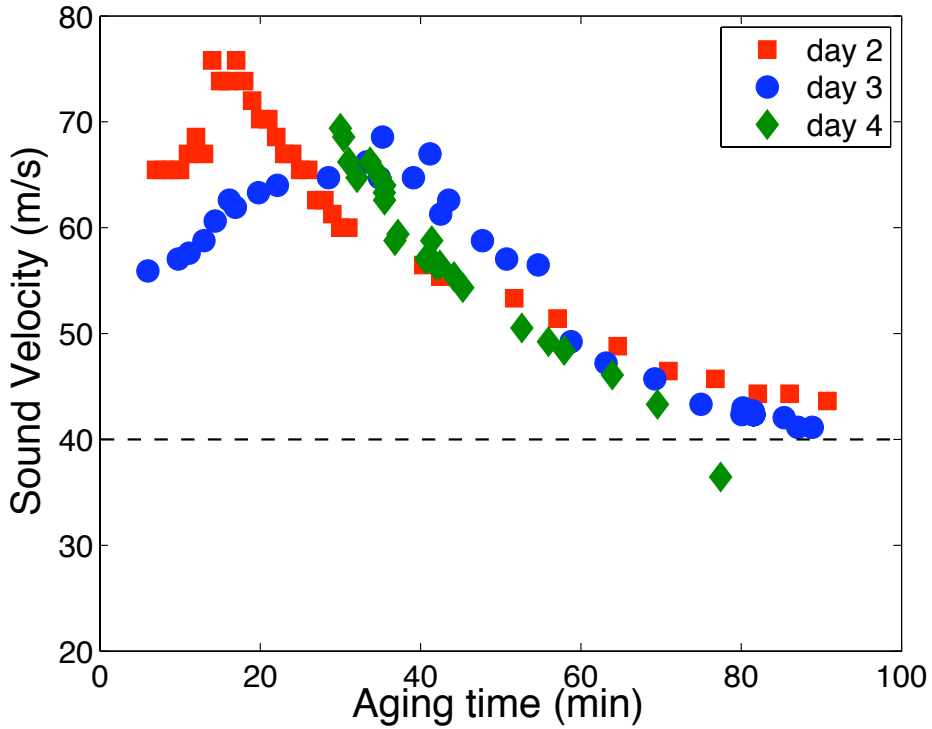

$L \approx 30$ cm $\quad D \approx 4$ cm $\quad f = 1$ kHz $\quad \lambda \approx 5$ cm

Part 2: Towards dislocation density measurement in solids (Resonant Ultrasound Spectroscopy)

Dislocations in solids: crystalline defects

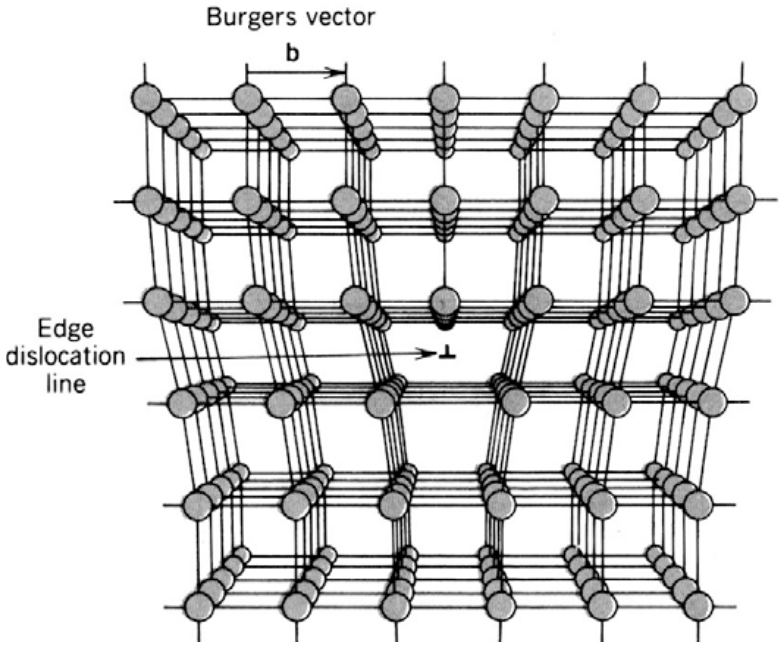

Dislocations produce a stress field that decays at long distances.

An oscillating dislocation radiates stress.

The energy to create a dislocations dictates if a material is brittle or ductile (plasticity).

Part 2: Towards dislocation density measurement in solids (Resonant Ultrasound Spectroscopy)

Dislocations in solids: crystalline defects

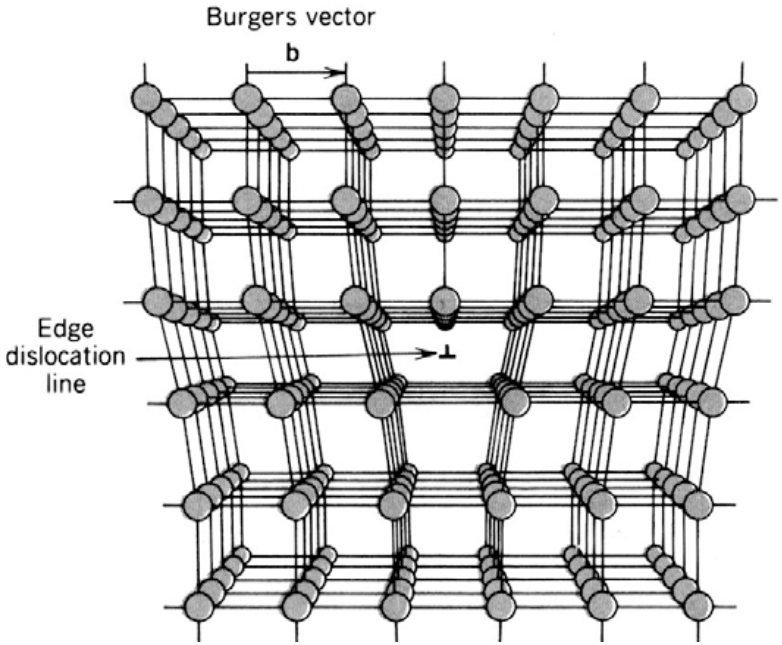

Dislocations produce a stress field that decays at long distances.

An oscillating dislocation radiates stress.

The energy to create a dislocations dictates if a material is brittle or ductile (plasticity).

Our objective: measure in a non-invasive way (ultrasound) the dislocation density in materials

Part 2: Towards dislocation density measurement in solids (Resonant Ultrasound Spectroscopy)

Collaborators & students

Fernando Lund & Felipe Barra (DFI, FCFM, Universidad de Chile)

Rodrigo Espinoza (DCM, FCFM, Universidad de Chile)

Alejandro Zuñiga (DIM, FCFM, Universidad de Chile)

Alejandro Jara & María Teresa Cerda (DFI, FCFM, Universidad de Chile)

Andrés Caru (Universidad Austral de Chile)

Part 2: Towards dislocation density measurement in solids (Resonant Ultrasound Spectroscopy)

Brittle versus fragile

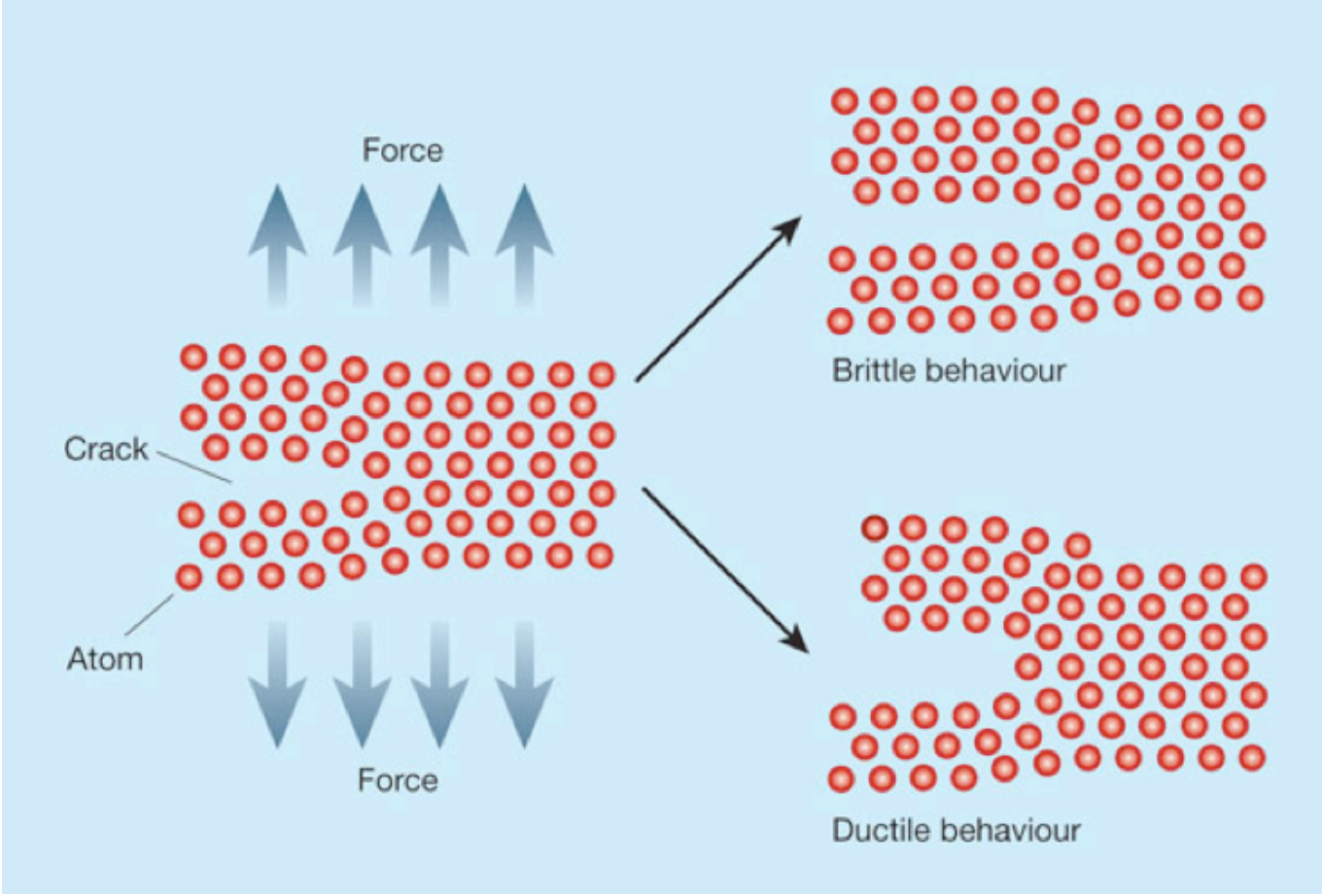

Part 2: Towards dislocation density measurement in solids (Resonant Ultrasound Spectroscopy)

Brittle versus fragile

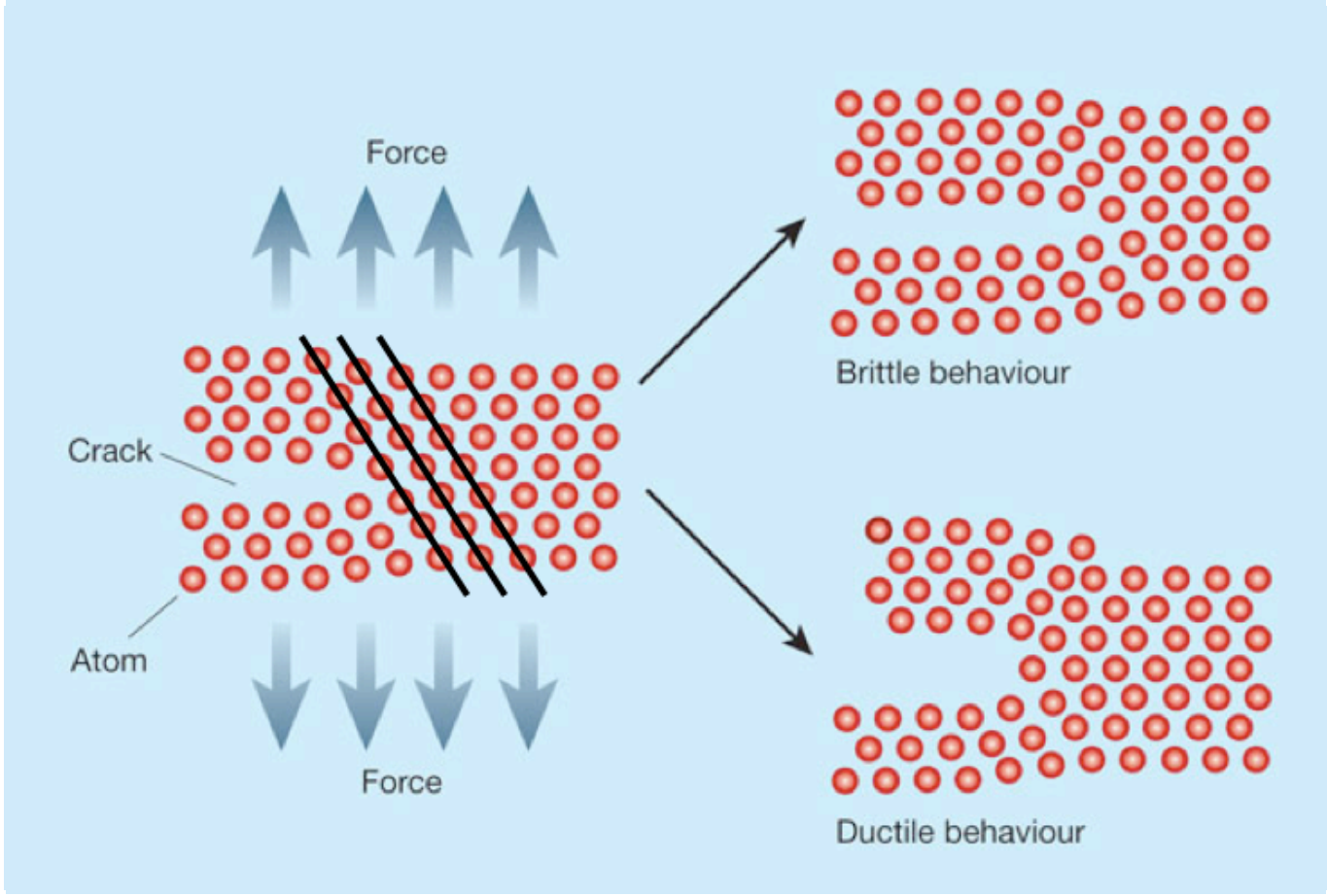

Part 2: Towards dislocation density measurement in solids (Resonant Ultrasound Spectroscopy)

Brittle versus fragile

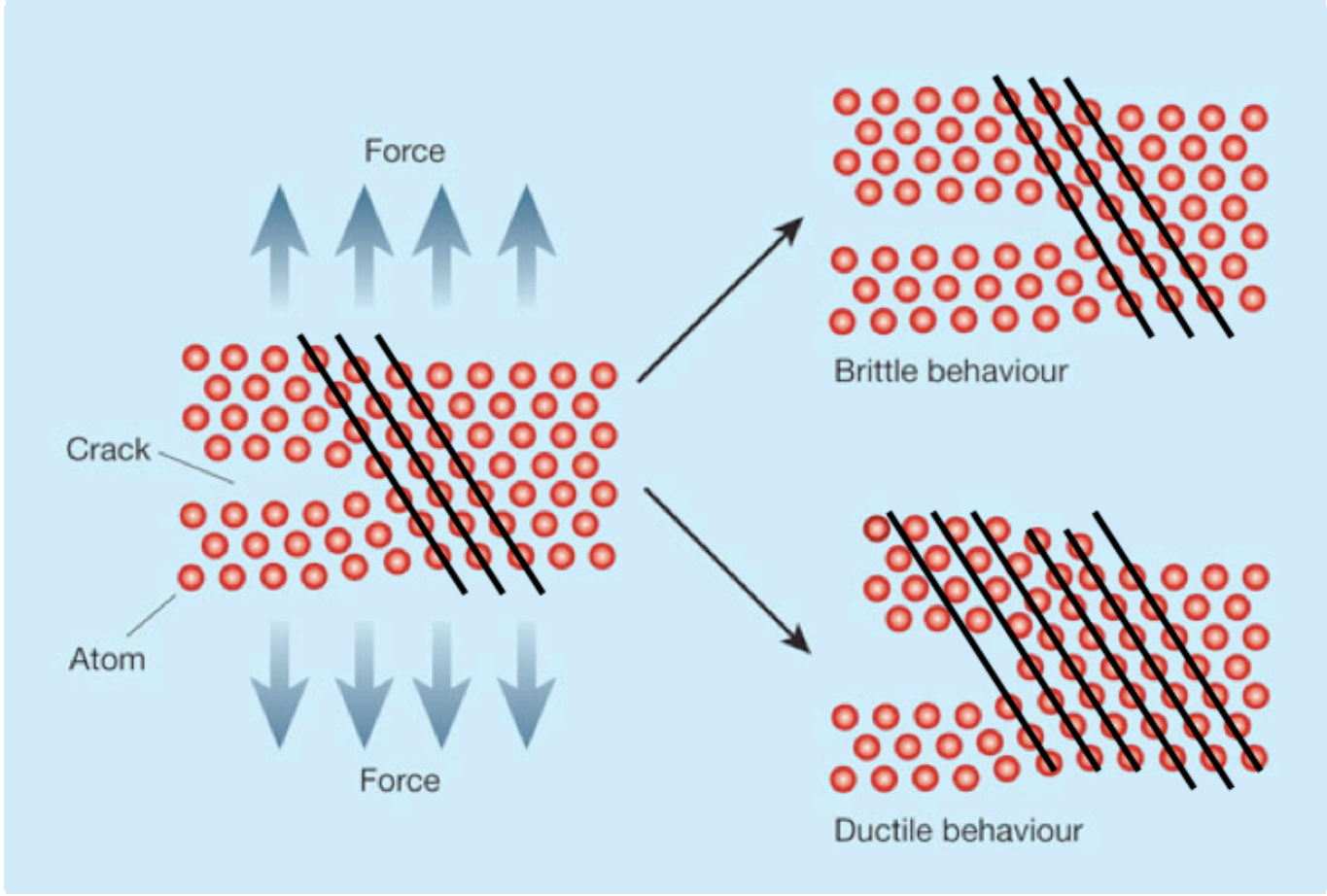

Sound-dislocation interaction

- Peach-Koehler force [1950]: dislocations are modeled as strings with fixed ends

$$m\ddot{X}(s,t) + B\dot{X}(s,t) - \Gamma X''(s,t) = F_{\rm PK}(t)$$

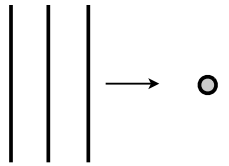

- Dislocations respond to the external force and act as sources of elastic waves

$$\rho\frac{\partial^2 v_i}{\partial t^2} - c_{ijkl}\frac{\partial^2 v_k}{\partial x_j \partial x_l} = s_i$$

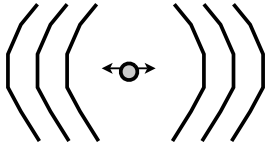

- The final result for a large number of randomly distributed dislocations

$$v_L = c_L\left(1 - \frac{16}{15\pi^4}\frac{1}{\gamma^2}\frac{\mu b^2}{\Gamma}\, nL^3\right)$$

$$v_T = c_T\left(1 - \frac{4}{5\pi^4}\frac{\mu b^2}{\Gamma}\, nL^3\right)$$

$n \equiv$ dislocations per unit volume

$L \equiv$ Typical distance between pinning points

- to be published in Int. J. of Bifurcation and Chaos (2009). arXiv:0808.1561

Sound-dislocation interaction

- Peach-Koehler force [1950]: dislocations are modeled as strings with fixed ends

$$m\ddot{X}(s,t) + B\dot{X}(s,t) - \Gamma X''(s,t) = F_{\rm PK}(t)$$

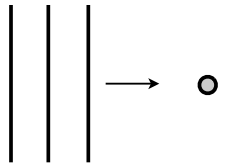

- Dislocations respond to the external force and act as sources of elastic waves

$$\rho\frac{\partial^2 v_i}{\partial t^2} - c_{ijkl}\frac{\partial^2 v_k}{\partial x_j \partial x_l} = s_i$$

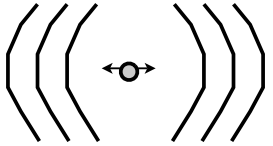

- The final result for a large number of randomly distributed dislocations

$$v_L = c_L\left(1 - \frac{16}{15\pi^4}\frac{1}{\gamma^2}\frac{\mu b^2}{\Gamma}\boxed{nL^3}\right)$$

$$v_T = c_T\left(1 - \frac{4}{5\pi^4}\frac{\mu b^2}{\Gamma}\boxed{nL^3}\right)$$

$n \equiv$ dislocations per unit volume

$L \equiv$ Typical distance between pinning points

- to be published in Int. J. of Bifurcation and Chaos (2009). arXiv:0808.1561

Aluminum 1100 samples (99.0% pure)

Transmission electron microscope (TEM) images

➡ Annealed sample (10 hrs)

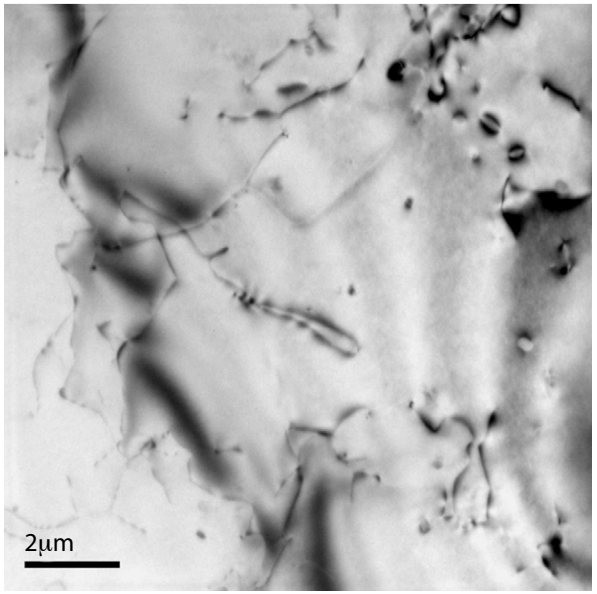

➡ Original sample

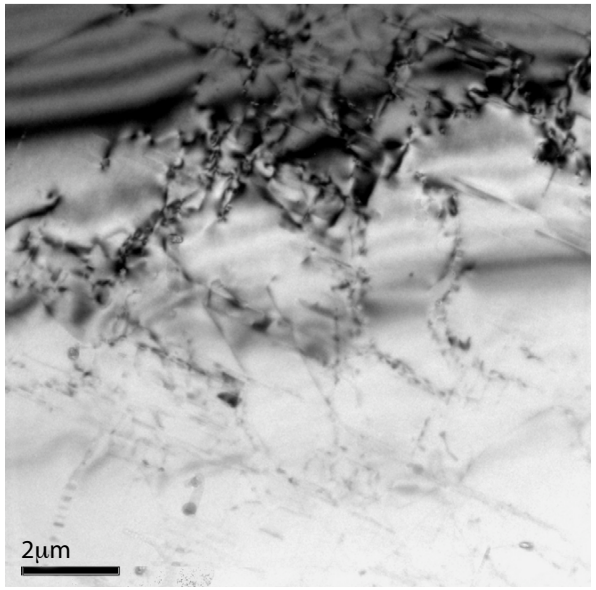

➡ Cold rolled sample 33%

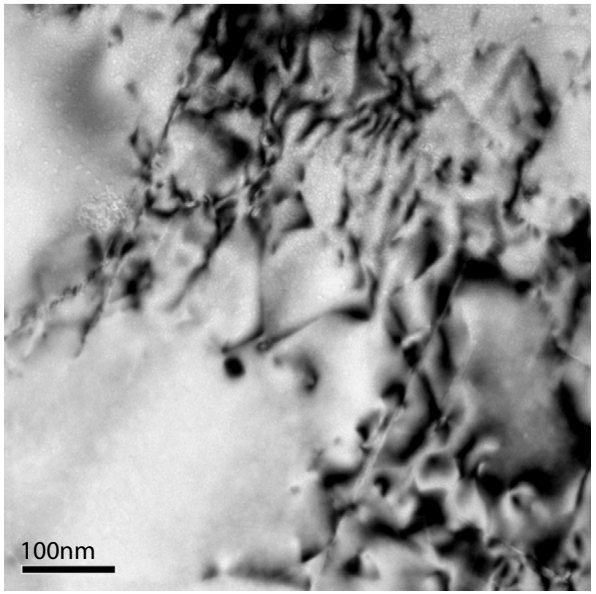

Aluminum 1100 samples (99.0% pure)

- Five parallelepiped samples were cut from the same aluminum bar

- Dislocation density measurements (TEM) and sample preparation was done by Rodrigo Espinoza (Material Science Department, FCFM, Universidad de Chile)

Sample Nº	Preparation	Dislocation density (mm^{-2})	Error (mm^{-2})
1	Annealed 400 C, 10 hrs	$2.7x10^6$	$6.8x10^5$
2	Annealed 400 C, 5 hrs	$2.3x10^7$	$1.8x10^7$
3	Original	$1.3x10^7$	$1.4x10^7$
4	Cold rolled 33%	$2.8x10^8$	$1.8x10^8$
5	Cold rolled 43%	in process	in process

Resonant Ultrasound Spectroscopy (RUS)

- Simple case: string with fixed boundary conditions
- Another simple case: Long and thin elastic bar
- In both cases theoretical formula are known for resonant frequencies. Their measurement could be used for material property characterization

$$f_n = \frac{n}{2L}\sqrt{\frac{T}{\rho}}$$

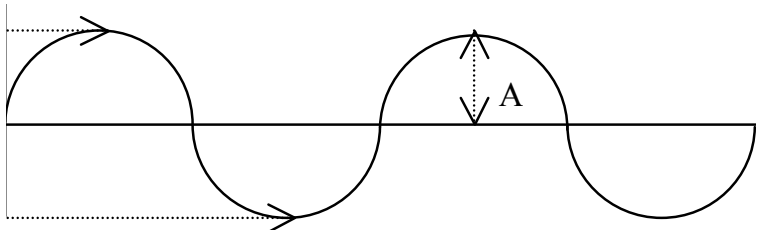

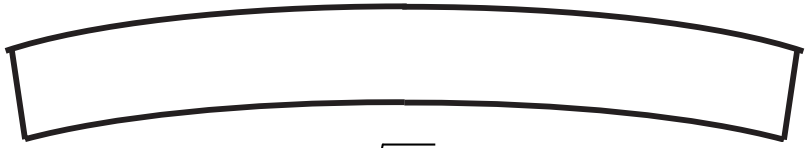

$$f_n^L = \sqrt{\frac{E}{\rho}}\frac{n}{2L}$$

$$f_n^B = \frac{\pi R}{16L^2}\sqrt{\frac{E}{\rho}}\cdot(2n+1)^2$$

$$f_n^T = \sqrt{\frac{E}{2\rho(1+\nu)}}\frac{n}{2L}$$

RUS: forward calculation

- For a 3D elastic solid, resonant frequencies can be obtained with the elastic wave equation:

$$C_{ijkl}\frac{\partial^2 u_k}{\partial x_j \partial x_l} = \rho\frac{\partial^2 u_i}{\partial t^2}$$

- Using the Rayleigh-Ritz expansion

$$u_i = \sum_\lambda a_{i,\lambda}\phi_\lambda$$

- The following matrix equation is obtained

$$\omega^2 \vec{E}\vec{a} = \vec{\Gamma}\vec{a}$$

- where

$$\vec{E} = \delta_{i,i'}\int_V \phi_\lambda \rho \phi_{\lambda'} dV \qquad \vec{\Gamma} = \sum_{j\,j'} C_{iji'j'}\int_V \frac{\partial\phi_\lambda}{\partial x_j}\frac{\partial\phi_{\lambda'}}{\partial x_{j'}} dV$$

- This approach neglects dissipation + Free boundary conditions!

RUS: forward calculation

7 11 12 15 16 18

Robert Leisure's group, http://www.physics.colostate.edu/groups/ultrasound/resonant-ultrasound.htm

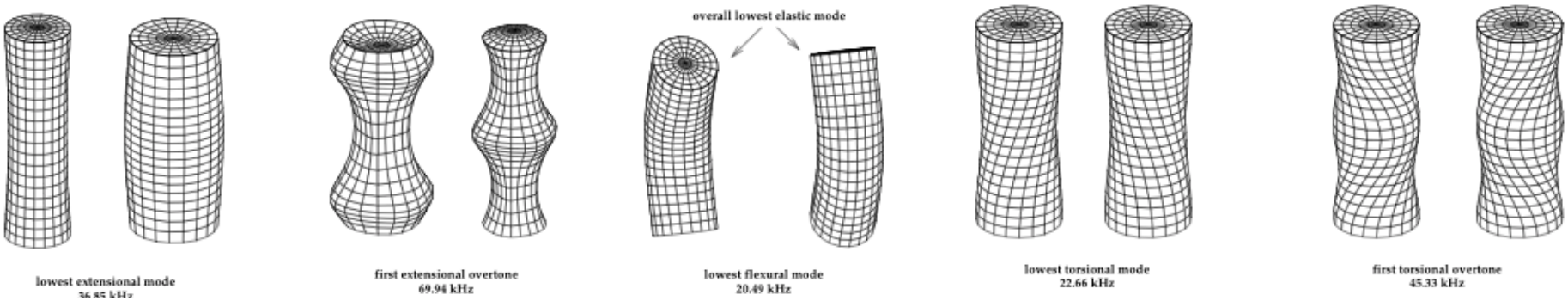

Extensional modes Bending modes Torsional modes

Brian Zadler's Ph.D. Dissertation

RUS: forward calculation

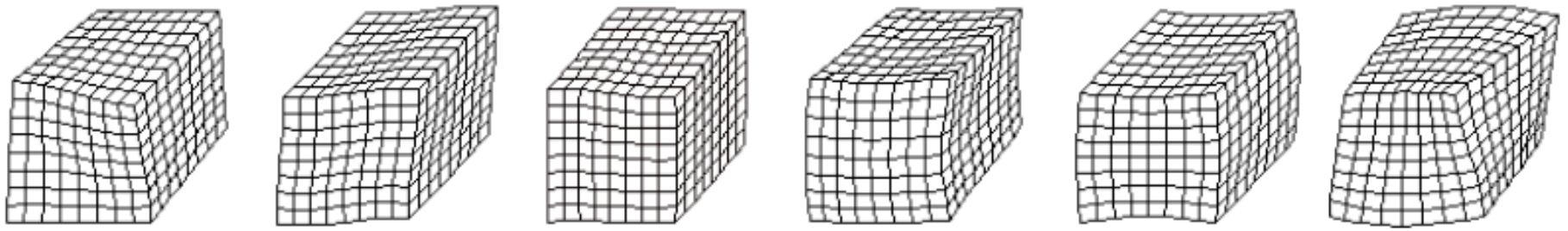

Robert Leisure's group, http://www.physics.colostate.edu/groups/ultrasound/resonant-ultrasound.htm

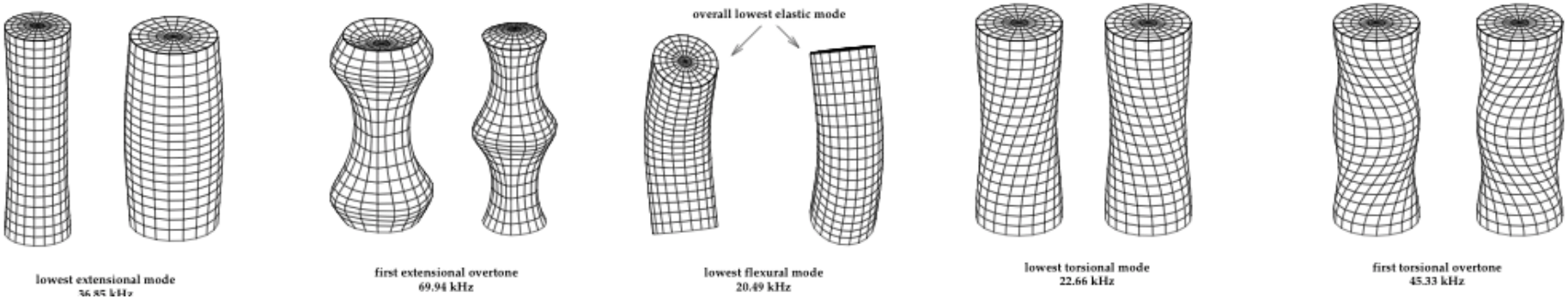

Extensional modes Bending modes Torsional modes

Brian Zadler's Ph.D. Dissertation

RUS: inverse calculation

- The goal is to minimize the objective function

$$\chi^2 = \sum_n w_n \frac{(f_n(a,b) - g_n)^2}{g_n^2}$$

- where $f_n(a,b)$ are the predicted frequencies
- g_n are the measured frequencies
- w_n are weight factors

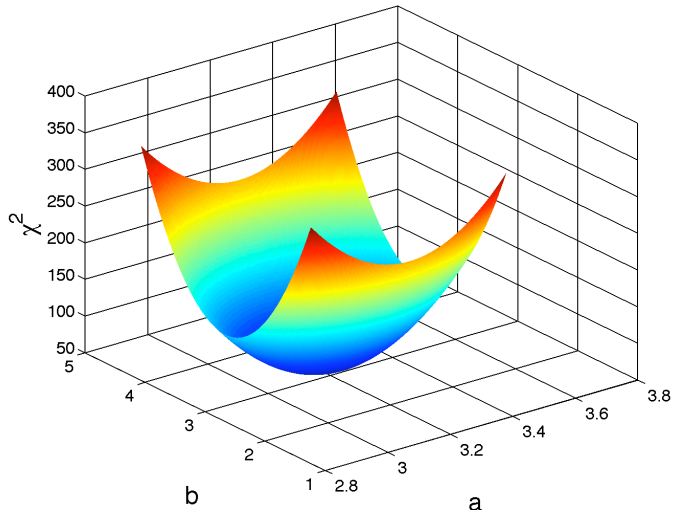

Some important names: Anderson, Migliori, Sarrao, Maynard, Leisure, Ogi...

Free code available at http://www.magnet.fsu.edu/inhouseresearch/rus/index.html

RUS: inverse calculation

- The goal is to minimize the objective function

$$\chi^2 = \sum_n w_n \frac{(f_n(a,b) - g_n)^2}{g_n^2}$$

- where $f_n(a,b)$ are the predicted frequencies
- g_n are the measured frequencies
- w_n are weight factors

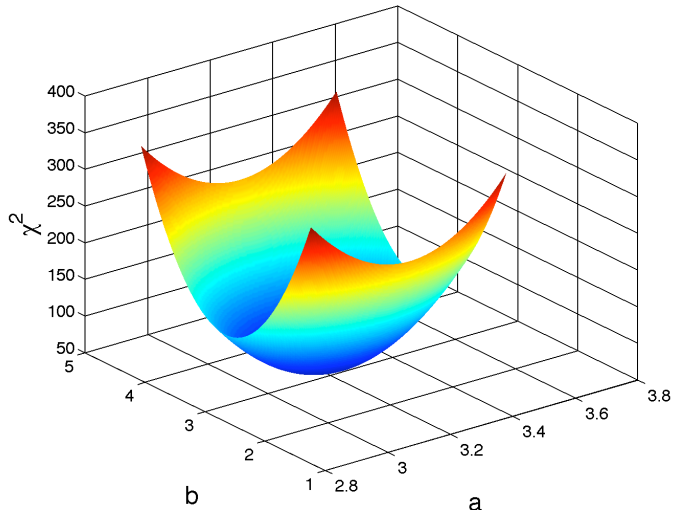

Some important names: Anderson, Migliori, Sarrao, Maynard, Leisure, Ogi...

Free code available at http://www.magnet.fsu.edu/inhouseresearch/rus/index.html

RUS allows to make measurements of material properties in a non-invasive way

Aluminum 1100 samples (99.0% pure)

- Mass density has to be measured precisely
- Opposite sides are parallel within 0.06º; adjacent sides are orthogonal within 0.3º. Sample can be safely modelled as ideal parallelepipeds [Spoor, 1996].
- Sample size insures homogeneity.

Parámetro	Muestra 1	Muestra 2	Muestra 3	Muestra 4	Muestra 5
	Annealed 400 C 5 hrs	Annealed 400 C 10 hrs	Original	Cold rolled 33%	Cold rolled 43%
d_1 [cm]	1.701 ± 0.001	1.700 ± 0.001	1.7011 ± 0.0002	1.696 ± 0.001	1.701 ± 0.001
d_2 [cm]	1.0015 ± 0.0002	0.9997 ± 0.0004	0.9998 ± 0.0003	1.001 ± 0.001	1.001 ± 0.001
d_3 [cm]	4.902 ± 0.001	4.900 ± 0.001	4.901 ± 0.001	4.901 ± 0.001	4.900 ± 0.001
M [g]	22.45 ± 0.01	22.38 ± 0.01	22.43 ± 0.01	22.35 ± 0.01	22.42 ± 0.01
ρ [g/cm^3]	2.688 ± 0.002	2.687 ± 0.002	2.691 ± 0.002	2.687 ± 0.004	2.687 ± 0.003

RUS Setup

- Sample contact force is small, about 0.1 N ≈ 1/2 sample weight ≈ 0.22 N
- With a SRS Spectrum Analyzer the first 13 resonant frequencies are measured. Since recently, up to 30 resonant frequencies can be measured.
- High Q values (>1000). Dissipation is negligible.
- Each resonant frequency is measured for five ultrasonic driving amplitudes to verify that the resonances are in the linear acoustic regime.
- Each sample is placed five times in the apparatus in order to reduce errors due to slight dependence on the contact load and positioning with respect to the ultrasonic receiver.

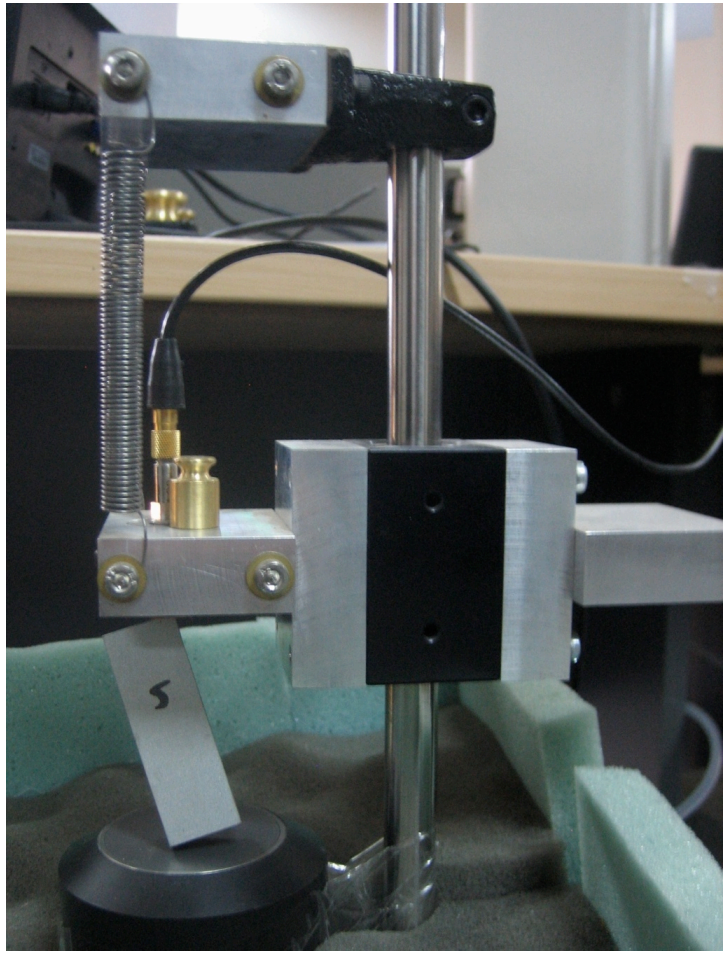

RUS Setup

- Sample contact force is small, about 0.1 N ≈ 1/2 sample weight ≈ 0.22 N
- With a SRS Spectrum Analyzer the first 13 resonant frequencies are measured. Since recently, up to 30 resonant frequencies can be measured.
- High Q values (>1000). Dissipation is negligible.
- Each resonant frequency is measured for five ultrasonic driving amplitudes to verify that the resonances are in the linear acoustic regime.
- Each sample is placed five times in the apparatus in order to reduce errors due to slight dependence on the contact load and positioning with respect to the ultrasonic receiver.

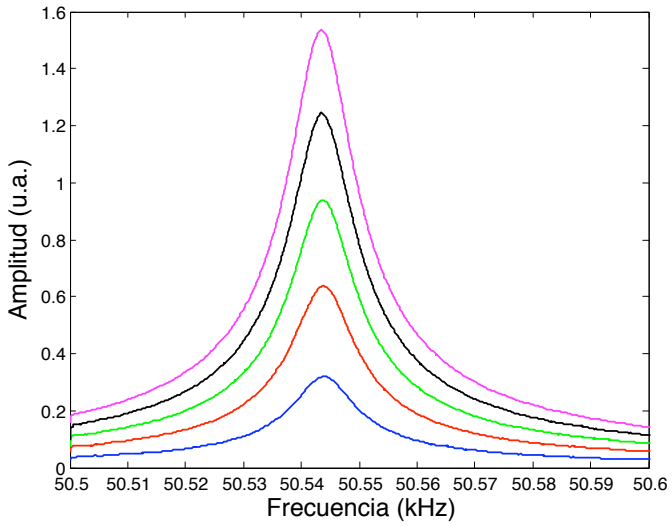

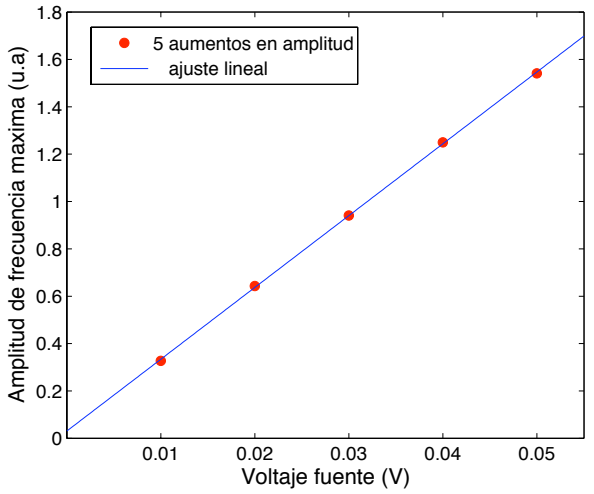

Results: Isotropic and homogenous samples

- Forward calculation using Ogi's data:
  C_{11} = 109.26 GPa & C_{44} = 26.72 GPa

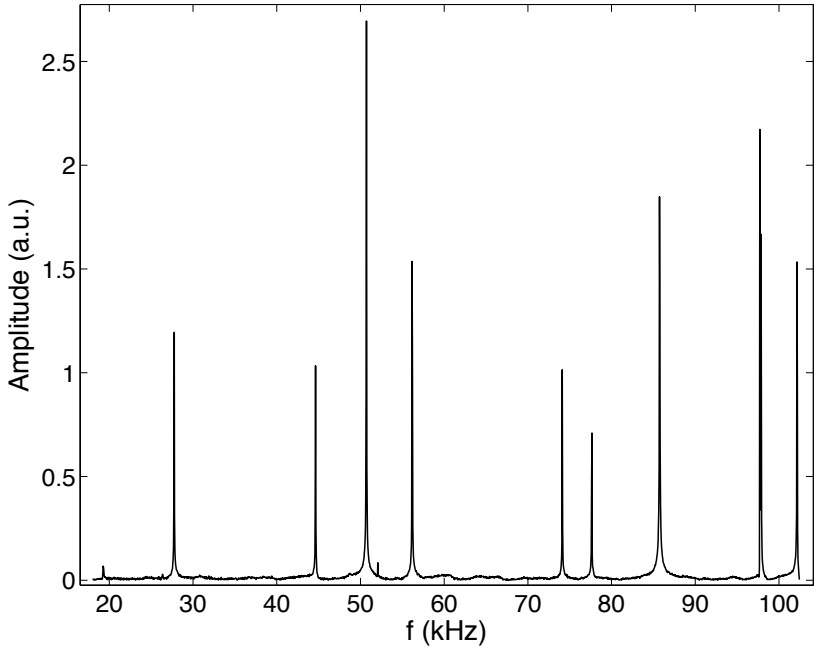

Inverse convergence:

C_{11}= 81.6±1.9 GPa ; C_{44} = 27.2±0.1 GPa

n	f_{exp} (kHz)	f_{cal} (kHz)	%err
1	19,387	19,485	0,51
2	26,468	25,899	-2,15
3	27,756	28,193	1,57
4	44,685	45,443	1,70
5	50,721	51,647	1,83
6	52,124	52,187	0,12
7	56,192	56,808	1,10
8	74,130	75,183	1,42
9	77,679	77,354	-0,42
10	85,763	86,370	0,71
11	97,725	97,309	-0,43
12	97,862	100,791	2,99
13	102,150	102,904	0,74
		RMS %err	1,45

Polycrystalline grain texture

- Sample 3: polycrystalline with grain size of about 540 μm x 460 μm.
- Another one cold-rolled at 20%: Grain size changes to 680 μm x 400 μm.

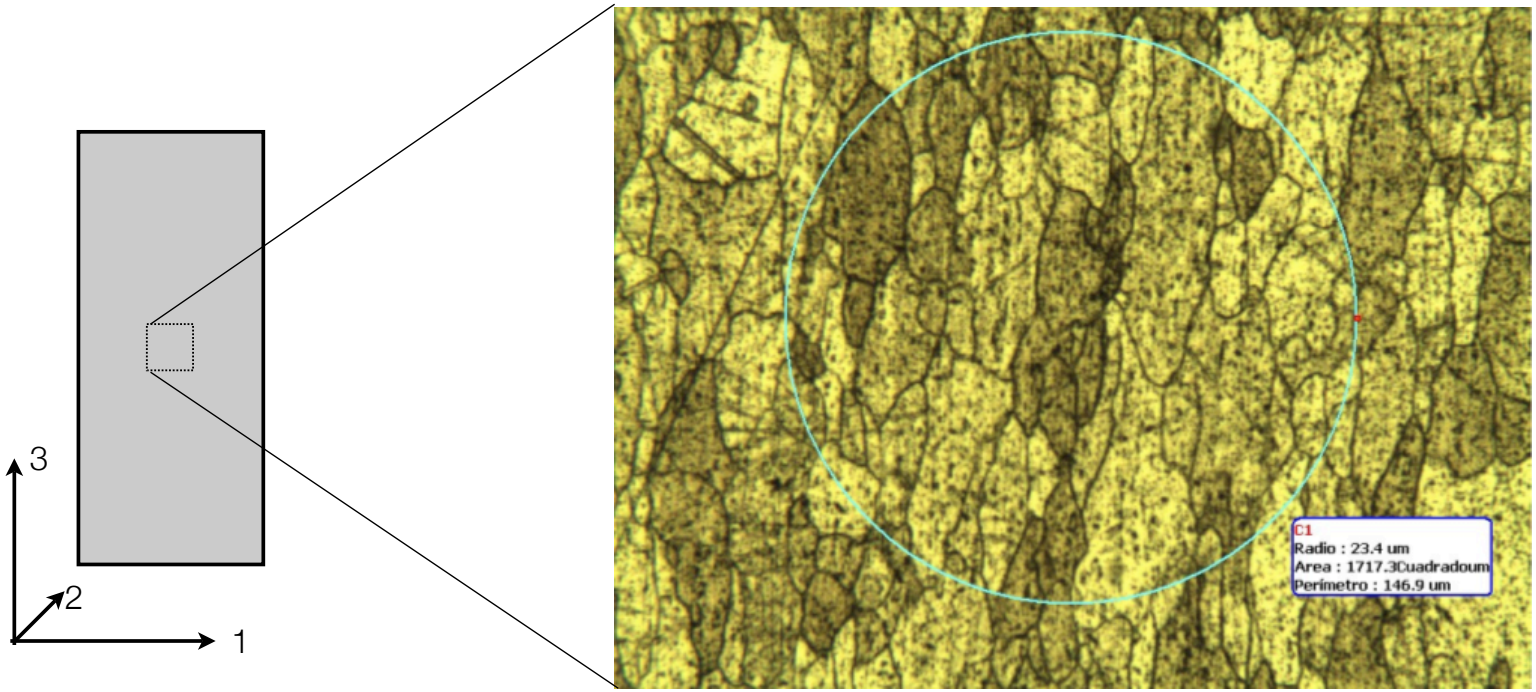

Polycrystalline grain texture

- Sample 3: polycrystalline with grain size of about 540 μm x 460 μm.
- Another one cold-rolled at 20%: Grain size changes to 680 μm x 400 μm.

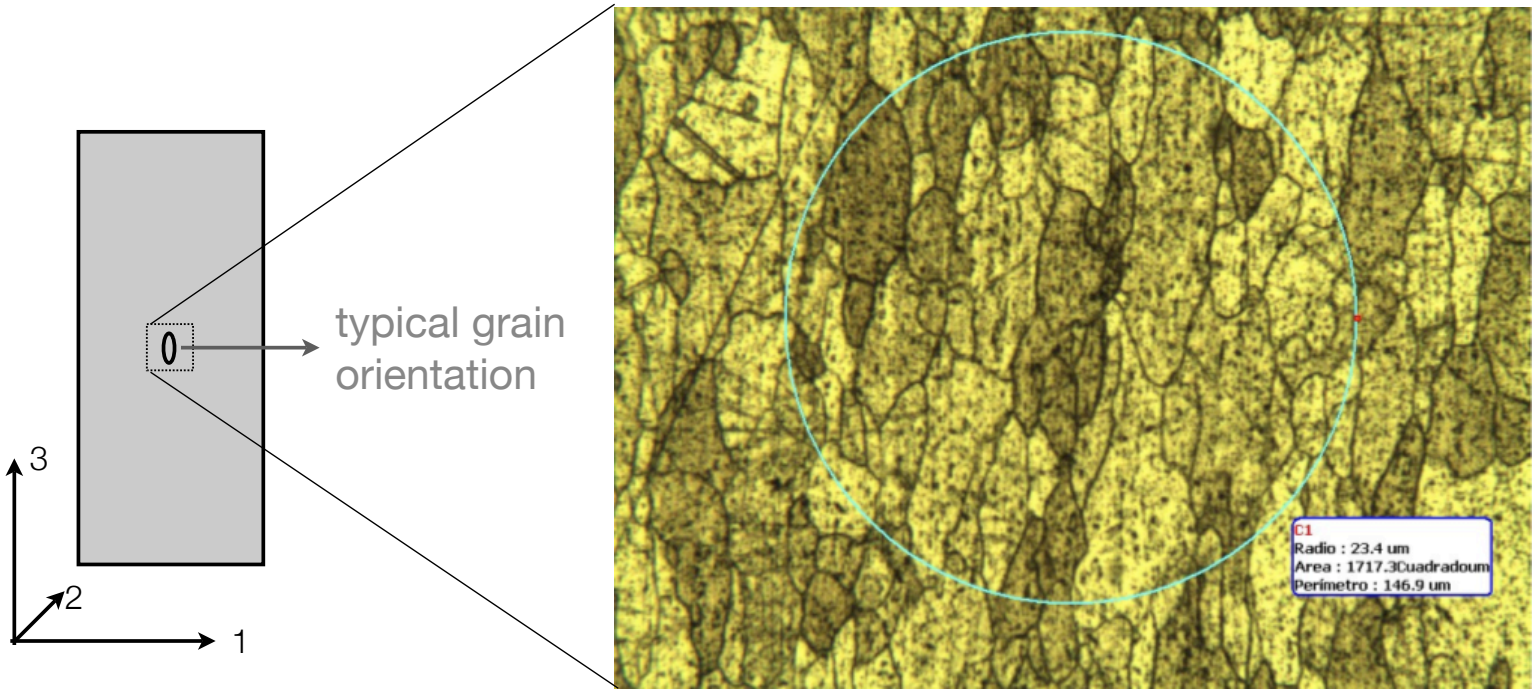

Isotropic or anisotropic?

- Because of the elongated nature of the polycrystalline grains, a plausible hypothesis is that our samples are slightly anisotropic: they might be transversly isotropic [Schwarz & Vuorinen, 2000]

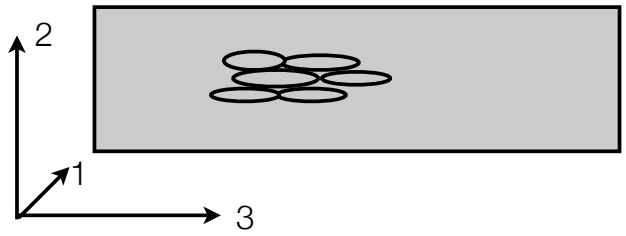

- In this sample spectra should be fitted with 5 independent elastic constants: C_{33}, C_{12}, C_{13}, C_{44}, & C_{66}
- In order to fit 5 elastic constants, up to ≈30 frequencies have been measured

Results

- Elastic constants:

Parámetro	Muestra 1	Muestra 2	Muestra 3	Muestra 4	Muestra 5
	Annealed 400 C 5 hrs	Annealed 400 C 10 hrs	Original	Cold rolled 33%	Cold rolled 43%
C_{11} (10^{11} Pa)	1.10 ± 0.04	1.12 ± 0.04	1.11 ± 0.05	1.19 ± 0.04	1.14 ± 0.03
C_{33} (10^{11} Pa)	1.12 ± 0.03	1.14 ± 0.03	1.13 ± 0.03	1.17 ± 0.03	1.14 ± 0.03
C_{23} (10^{11} Pa)	0.61 ± 0.03	0.63 ± 0.03	0.62 ± 0.04	0.68 ± 0.04	0.64 ± 0.03
C_{12} (10^{11} Pa)	0.59 ± 0.04	0.60 ± 0.04	0.60 ± 0.05	0.69 ± 0.04	0.62 ± 0.03
C_{44} (10^{11} Pa)	0.2745 ± 0.0002	0.2728 ± 0.0002	0.2738 ± 0.0002	0.2712 ± 0.0002	0.2697 ± 0.0001

- Samples are indeed slightly anisotropic: measurements are consistent with transverse isotropy

$$\varepsilon = 1 - \frac{2C_{44}}{C_{11} - C_{12}} \qquad \varepsilon' = 1 - \frac{C_{11}}{C_{33}} \qquad \varepsilon'' = 1 - \frac{C_{44}}{C_{66}}$$

Parámetro	Muestra 1	Muestra 2	Muestra 3	Muestra 4	Muestra 5
ε	-0.1 ± 0.1	-0.1 ± 0.1	-0.1 ± 0.2	-0.1 ± 0.1	-0.04 ± 0.08
ε'	0.02 ± 0.04	0.02 ± 0.04	0.02 ± 0.05	-0.02 ± 0.04	0.01 ± 0.04
ε''	-0.056 ± 0.008	-0.045 ± 0.008	-0.065 ± 0.008	-0.072 ± 0.004	-0.054 ± 0.004

➡ We can compare with isotropic theory

Results

- C_{11} & C_{44} are very close to previously published results for isotropic Aluminum
- Errors for C_{11} are large (~5%); for C_{44} they are small (~0.1%)
- Velocity measurements:

Parámetro	Muestra 1	Muestra 2	Muestra 3	Muestra 4	Muestra 5
	Annealed 400 C 5 hrs	Annealed 400 C 10 hrs	Original	Cold rolled 33%	Cold rolled 43%
V_L (m/s)	6410 ± 111	6458 ± 102	6429 ± 140	6662 ± 112	6504 ± 90
V_T (m/s)	3195 ± 2	3186 ± 2	3190 ± 2	3176 ± 3	3168 ± 2

$$v_L = \sqrt{\frac{C_{11}}{\rho}} \qquad v_T = \sqrt{\frac{C_{44}}{\rho}}$$

Results

- C_{44} and v_T show a decreasing trend as function of dislocation density

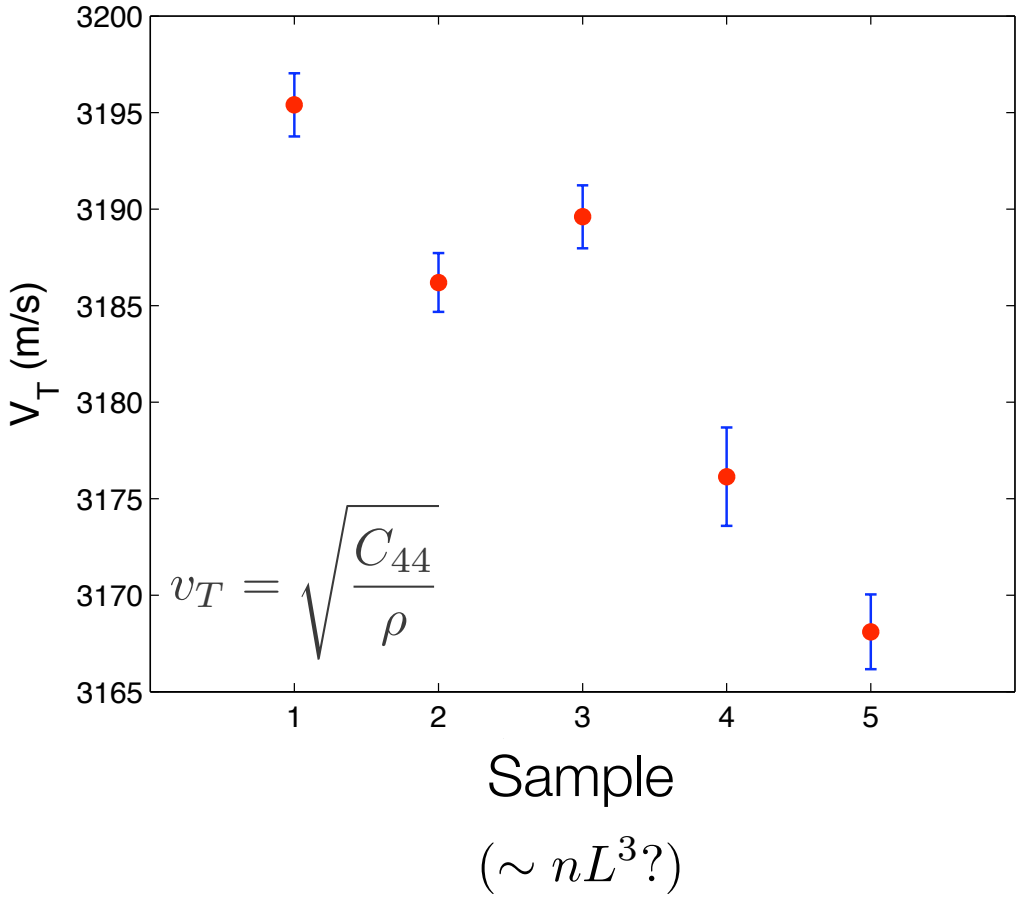

Results

- Correlation with TEM measurements

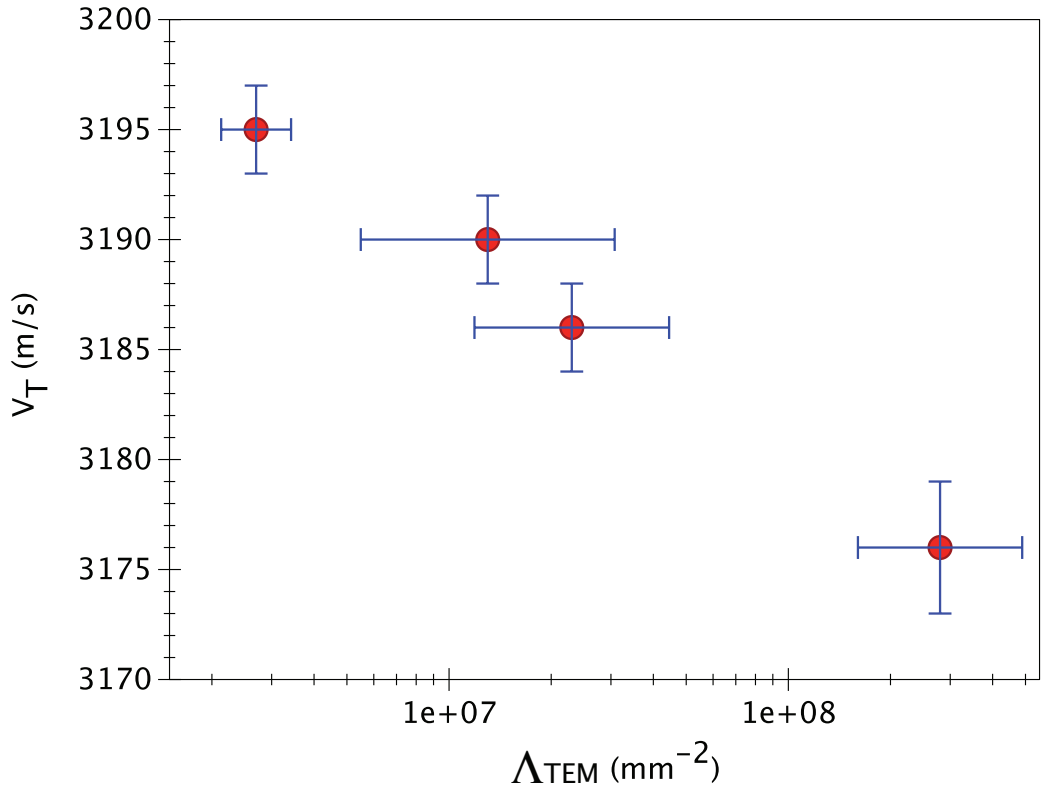

Summary part 2

- Extrudend 1100 Al samples are indeed slightly anisotropic: they present transverse isotropy. Comparison with theory for isotropic medium is possible
- Our C_{11} & C_{44} are very close to previously published results
- As predicted, C_{44} and v_T show a decreasing trend as function of “dislocation density”
- Actually, nL^3 must be obtained with TEM measurements in order to fully correlate measurements with theory (work in progress)
- Nonlinear resonances will serve to obtain intrinsic nonlinear parameters that could be more sensitive to dislocation density